Schnabel

Hole: C-714
Location:C C N P P

Cone:STD 20T AD-195
Date:07:19:06 14:19

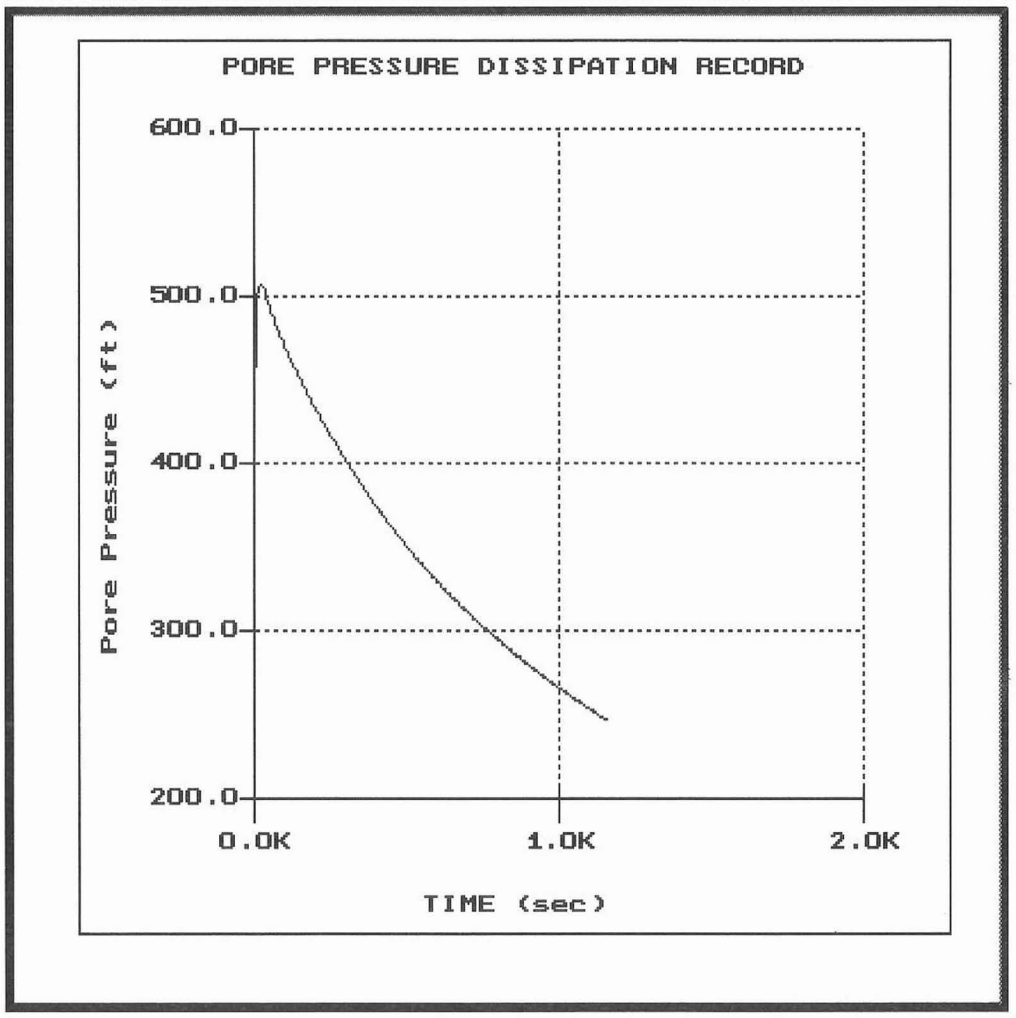

File: 948CP37.PPD
Depth (m): 17.40
(ft): 57.09
Duration : 1160.0s
U-min: 246.66 1160.0s
U-max: 507.48 20.0s

Schnabel

Hole: C-717
Location:C C N P P

Cone:STD 20T AD-195
Date:07:19:06 07:39

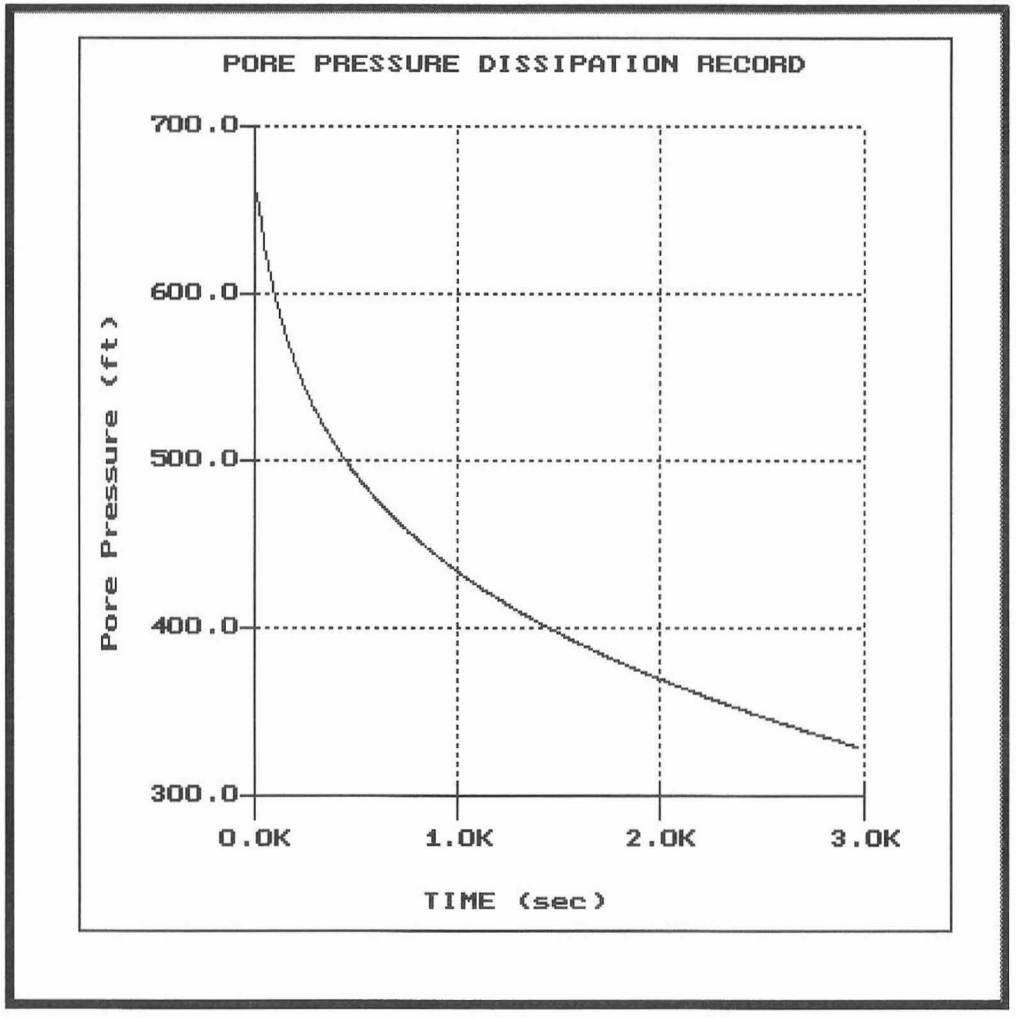

File: 948CP33.PPD
Depth (m): 15.50
(ft): 50.85
Duration : 2970.0s
U-min: 328.97 2970.0s
U-max: 661.60 5.0s

Schnabel

Hole: C-720
Location:C C N P P

Cone:STD 20T AD-195
Date:07:20:06 08:17

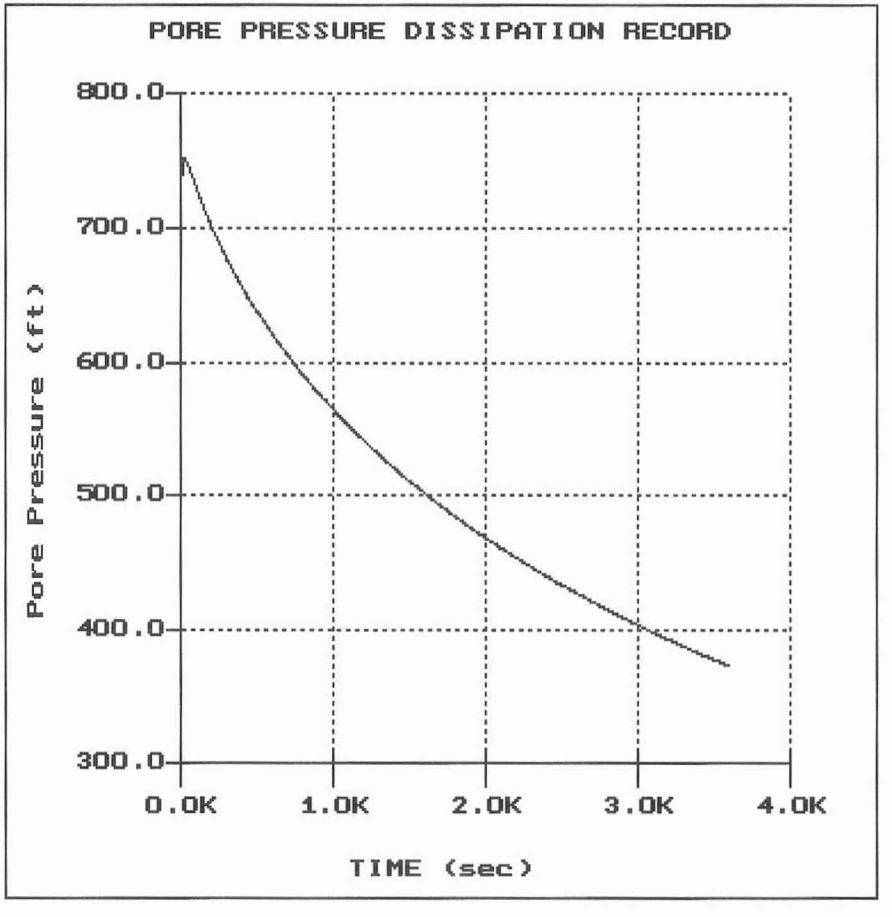

File: 948CP39.PPD
Depth (m): 15.75
(ft): 51.67
Duration : 3590.0s
U-min: 372.57 3590.0s
U-max: 751.61 20.0s

Schnabel

Hole: C-723
Location:C C N P P

Cone:STD 20T AD-195
Date:07:18:06 07:35

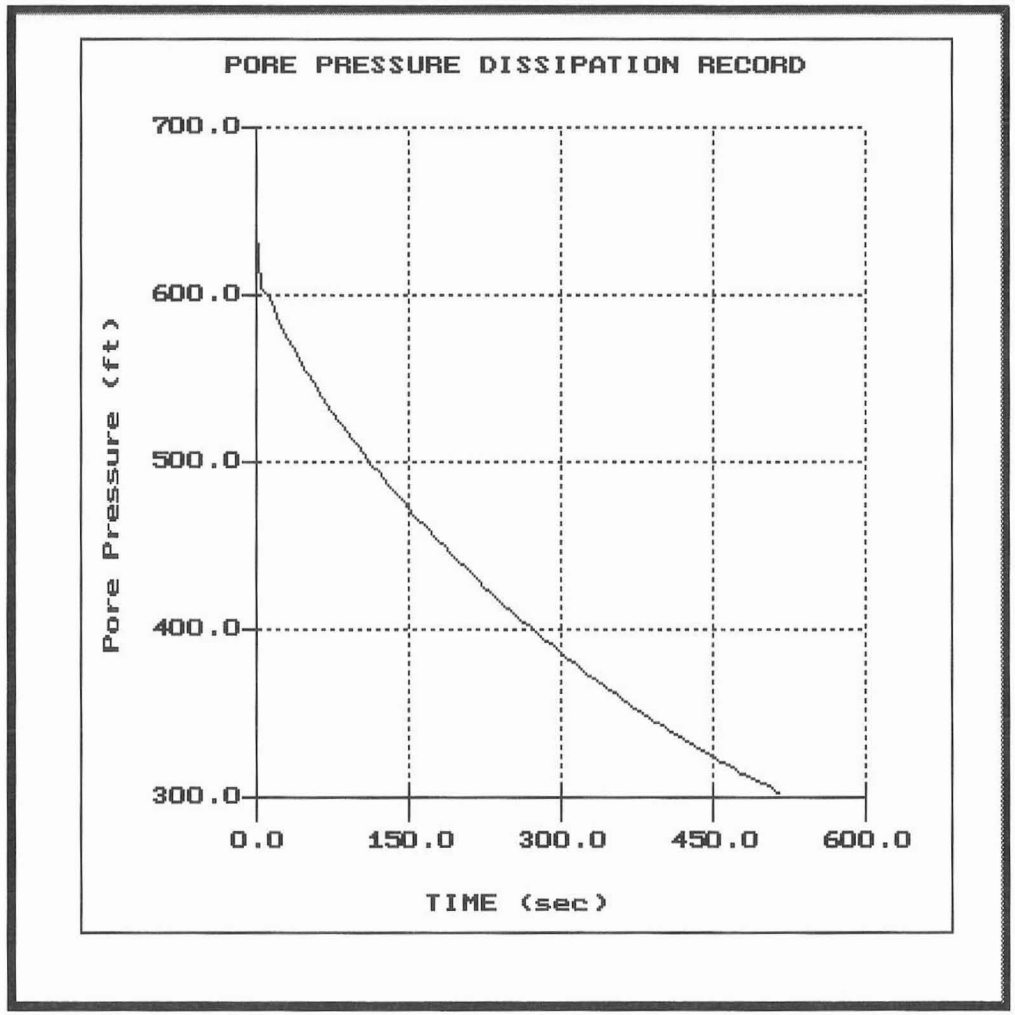

File: 948CP26.PPD
Depth (m): 11.75
(ft): 38.55
Duration : 515.0s
U-min: 302.64 515.0s
U-max: 640.67 0.0s

APPENDIX D
CPT INTERPRETATION METHODS

Presentation of In Situ Testing Program Results
ConeTec, Inc.
November 13, 2006

ConeTec Interpretations as of June 30, 2004 (Release 1.22A)

ConeTec's interpretation routine provides a tabular output of geotechnical parameters based on current published CPT correlations and is subject to change to reflect the current state of practice. The interpreted values are not considered valid for all soil types. The interpretations are presented only as a guide for geotechnical use and should be carefully scrutinized for consideration in any geotechnical design. Reference to current literature is strongly recommended. ConeTec does not warranty the correctness or the applicability of any of the geotechnical parameters interpreted by the program and does not assume liability for any use of the results in any design or review. Representative hand calculations should be made for any parameter that is critical for design purposes. The end user of the interpreted output should also be fully aware of the techniques and the limitations of any method used in this program. The purpose of this document is to inform the user as to which methods were used and what the appropriate papers and/or publications are for further reference.

The CPT interpretations are based on values of tip, sleeve friction and pore pressure averaged over a user specified interval (e.g. 0.20m). Note that q_t is the tip resistance corrected for pore pressure effects and q_c is the recorded tip resistance. Since all ConeTec cones have equal end area friction sleeves, pore pressure corrections to sleeve friction, f_s, are not required.

The tip correction is: $q_t = q_c + (1-a) \bullet u_2$

where: q_t is the corrected tip resistance
q_c is the recorded tip resistance
u_2 is the recorded dynamic pore pressure behind the tip (u_2 position)
a is the Net Area Ratio for the cone (typically 0.85 for ConeTec cones)

The total stress calculations are based on soil unit weights that have been assigned to the Soil Behavior Type zones, from a user defined unit weight profile or by using a single value throughout the profile. Effective vertical overburden stresses are calculated based on a hydrostatic distribution of equilibrium pore pressures below the water table or from a user defined equilibrium pore pressure profile (this can be obtained from CPT dissipation tests). For over water projects the effects of the column of water have been taken into account as has the appropriate unit weight of water. How this is done depends on where the instruments were zeroed (i.e. on deck or at mud line).

Details regarding the interpretation methods for all of the interpreted parameters are provided in Table 1. The appropriate references cited in Table 1 are listed in Table 2. Where methods are based on charts or techniques that are too complex to describe in this summary the user should refer to the cited material.

The estimated Soil Behavior Types (normalized and non-normalized) are based on the charts developed by Robertson and Campanella shown in Figures 1 and 2. The Bq classification charts are not reproduced in this document but can be reviewed in Lunne, Robertson and Powell (1997) or Robertson (1990).

Where the results of a calculation/interpretation are declared *'invalid'* the value will be represented by the text strings "-9999" or "-9999.0". In some cases the value 0 will be used. Invalid results will occur because of (and not limited to) one or a combination of:

1. Invalid or undefined CPT data (e.g. drilled out section or data gap).

2. Where the interpretation method is inappropriate, for example, drained parameters in an undrained material (and vice versa).

3. Where interpretation input values are beyond the range of the referenced charts or specified limitations of the interpretation method.

4. Where pre-requisite or intermediate interpretation calculations are invalid.

The parameters selected for output from the program are often specific to a particular project. As such, not all of the interpreted parameters listed in Table 1 may be included in the output files delivered with this report.

The output files are often delivered in one (or more) of the following three formats:

File Type	Typical Extensions	Description
Printable	IFP, NLP	ASCII files formatted for direct printing either by copying to a printer port, through a text editor or through a dedicated printing routine (such as ConeTec's CTPRINT). Typically formatted for 132 columns wide and 70 lines per page. Any printer would need to be set to have a compressed font (16cpi) as its default.
Importable	IFI, NLI	Tab delimited ASCII files (not for use with text editors) meant for importing into spreadsheet and database applications (e.g. Excel, Lotus, Quattro, Access). Some column and cell formatting maybe required depending on the quality of the application's import utility.
Spreadsheet	XLS	IFI, NLI files exported directly to Excel format. Column and cell formatting has been done. Header information is exported to start in Column C allowing the depth columns A and/or B to be duplicated on each printed page without repetition of part of the header information.

Table 1
CPT Interpretation Methods

Interpreted Parameter	Description	Equation	Ref
Depth	Mid Layer Depth *(where interpretations are done at each point then Mid Layer Depth = Recorded Depth)*	*Depth (Layer Top) + Depth (Layer Bottom) / 2.0*	
Elevation	Elevation of Mid Layer based on sounding collar elevation supplied by client	Elevation = Collar Elevation - Depth	
Avgqc	Averaged recorded tip value (q_c)	$Avgqc = \frac{1}{n}\sum_{i=1}^{n} q_c$ *n=1 when interpretations are done at each point*	
Avgqt	Averaged corrected tip (q_t) where: $q_t = q_c + (1-a) \bullet u$	$Avgqt = \frac{1}{n}\sum_{i=1}^{n} q_t$ *n=1 when interpretations are done at each point*	
Avgfs	Averaged sleeve friction (f_s)	$Avgfs = \frac{1}{n}\sum_{i=1}^{n} fs$ *n=1 when interpretations are done at each point*	
AvgRf	Averaged friction ratio (Rf) where friction ratio is defined as: $Rf = 100\% \bullet \frac{fs}{qt}$	$AvgRf = 100\% \bullet \frac{Avgfs}{Avgqt}$ *n=1 when interpretations are done at each point*	
Avgu	Averaged dynamic pore pressure *(u)*	$Avgu = \frac{1}{n}\sum_{i=1}^{n} u_i$ *n=1 when interpretations are done at each point*	
AvgRes	Averaged Resistivity (this data is not always available since it is a specialized test requiring an additional module)	$Avgu = \frac{1}{n}\sum_{i=1}^{n} RESISTIVITY_i$ *n=1 when interpretations are done at each point*	

Interpreted Parameter	Description	Equation	Ref
AvgUVIF	Averaged UVIF ultra-violet induced fluorescence (this data is not always available since it is a specialized test requiring an additional module)	$Avgu = \frac{1}{n}\sum_{i=1}^{n} UVIF_i$ *n=1 when interpretations are done at each point*	
AvgTemp	Averaged Temperature (this data is not always available since it is a specialized test)	$Avgu = \frac{1}{n}\sum_{i=1}^{n} TEMPERATURE_i$ *n=1 when interpretations are done at each point*	
AvgGamma	Averaged Gamma Counts (this data is not always available since it is a specialized test requiring an additional module)	$Avgu = \frac{1}{n}\sum_{i=1}^{n} GAMMA_i$ *n=1 when interpretations are done at each point*	
SBT	Soil Behavior Type as defined by Robertson and Campanella	See Figure 1	2, 5
U.Wt.	Unit Weight of soil determined from one of the following user selectable options: 1) uniform value 2) value assigned to each SBT zone 3) user supplied unit weight profile	See references	5
T. Stress σ_v	Total vertical overburden stress at Mid Layer Depth. *A layer is defined as the averaging interval specified by the user. For data interpreted at each point the Mid Layer Depth is the same as the recorded depth.*	$TStress = \sum_{i=1}^{n} \gamma_i h_i$ *where* γ_i is layer unit weight h_i is layer thickness	
E. Stress σ_v'	Effective vertical overburden stress at Mid Layer Depth	*Estress = Tstress - u_{eq}*	
Ueq	Equilibrium pore pressure determined from one of the following user selectable options: 1) hydrostatic from water table depth 2) user supplied profile	For hydrostatic option: $u_{eq} = \gamma_w \bullet (D - D_{wt})$ where u_{eq} is equilibrium pore pressure γ_w is unit weight of water D is the current depth D_{wt} is the depth to the water table	
Cn	SPT N_{60} overburden correction factor	*$Cn=(\sigma_v')^{-0.5}$* where *σ_v' is in tsf* *$0.5 < C_n < 2.0$*	
N_{60}	SPT N value at 60% energy calculated from qt/N ratios assigned to each SBT zone. This method has abrupt N value changes at zone boundaries.	*See Figure 1*	4, 5
$(N_1)_{60}$	SPT N_{60} value corrected for overburden pressure	*$(N_1)_{60} = Cn \bullet N_{60}$*	4
$N_{60}I_c$	SPT N_{60} values based on the Ic parameter	(qt/pa)/ N_{60} = 8.5 (1 – Ic/4.6)	5
$(N_1)_{60}$Ic	SPT N_{60} value corrected for overburden pressure (using N_{60} $I_{c)}$. User has 2 options.	*1) $(N_1)_{60}Ic = Cn \bullet (N_{60}\ Ic)$* 2) q_{c1n}/ *$(N_1)_{60}Ic$* = 8.5 (1 – Ic/4.6)	4 5
$(N_1)_{60cs}$Ic	Clean sand equivalent SPT $(N_1)_{60}$Ic. User has 3 options.	1) $(N_1)_{60cs}Ic = \alpha + \beta((N_1)_{60}Ic)$ 2) $(N_1)_{60cs}Ic = K_{SPT} * ((N_1)_{60}Ic)$ 3) q_{c1ncs}/ $(N_1)_{60cs}Ic$ = 8.5 (1 – Ic/4.6) FC ≤ 5%: α = 0, β=1.0 FC ≥ 35% α = 5.0, β=1.2 5% < FC < 35% α = exp[1.76 – (190/FC^2)] β = [0.99 + ($FC^{1.5}$/1000)]	10 10 5
Su	Undrained shear strength - N_{kt} is user selectable	$Su = \frac{qt - \sigma_v}{N_{kt}}$	1, 5
k	Coefficient of permeability (assigned to each SBT zone)		5

Interpreted Parameter	Description	Equation	Ref
Bq	Pore pressure parameter	$Bq = \frac{\Delta u}{qt - \sigma_v}$ *where:* $\Delta u = u - u_{eq}$ *and u = dynamic pore pressure* *u_{eq} = equilibrium pore pressure*	1, 5
Q_t	Normalized q_t for Soil Behavior Type classification as defined by Robertson, 1990	$Qt = \frac{qt - \sigma_v}{\sigma'_v}$	2, 5
F_r	Normalized Friction Ratio for Soil Behavior Type classification as defined by Robertson, 1990	$Fr = 100\% \bullet \frac{fs}{qt - \sigma_v}$	2, 5
SBTn	Normalized Soil Behavior Type as defined by Robertson and Campanella	See Figure 2	2, 5
SBT-BQ	Non-normalized soil behavior type based on the Bq parameter	See Figure 5.7 (reference 5)	2, 5
SBT-BQn	Normalized Soil Behavior base on the Bq parameter	See Figure 5.8 (reference 5) or Figure 3 (reference 2)	2, 5
I_c	Soil index for estimating grain characteristics	*$Ic = [(3.47 - \log_{10}Q)^2 + (\log_{10} Fr + 1.22)^2]^{0.5}$* *Where:* $Q = \left(\frac{qt - \sigma_v}{P_{a2}}\right)\left(\frac{P_a}{\sigma'_v}\right)^n$ *And Fr is in percent* *P_a = atmospheric pressure* *P_{a2} = atmospheric pressure* *n varies from 0.5 to 1.0 and is selected in an iterative manner based on the resulting I_c*	3, 8
FC	Apparent fines content (%)	*$FC=1.75(Ic^{3.25}) - 3.7$* *FC=100 for Ic > 3.5* *FC=0 for Ic < 1.26* *FC = 5% if 1.64 < Ic < 2.6 AND F_r<0.5*	3
Ic Zone	This parameter is the Soil Behavior Type zone based on the Ic parameter (valid for zones 2 through 7 on SBTn chart)	Ic < 1.31 Zone = 7 1.31 < Ic < 2.05 Zone = 6 2.05 < Ic < 2.60 Zone = 5 2.60 < Ic < 2.95 Zone = 4 2.95 < Ic < 3.60 Zone = 3 Ic > 3.60 Zone = 2	3
PHI ϕ	Friction Angle determined from one of the following user selectable options: a) Campanella and Robertson b) Durgunoglu and Mitchel c) Janbu	See reference	5
Dr	Relative Density determined from one of the following user selectable options: a) Ticino Sand b) Hokksund Sand c) Schmertmann 1976 d) Jamiolkowski - All Sands	See reference	5

Interpreted Parameter	Description	Equation	Ref
OCR	Over Consolidation Ratio	a) Based on Schmertmann's method involving a plot of S_u/σ_v' /($S_u/\sigma_v')_{NC}$ and OCR where the Su/p' ratio for NC clay is user selectable	9
State Parameter	The state parameter is used to describe whether a soil is contractive (SP is positive) or dilative (SP is negative) at large strains based on the work by Been and Jefferies	See reference	8, 6, 5
Es/qt	Intermediate parameter for calculating Youngs Modulus, E, in sands. It is the Y axis of the reference chart.	Based on Figure 5.59 in the reference	5
Youngs Modulus E	Youngs Modulus based on the work by Baldi. There are three types of sands considered in this technique. The user selects the appropriate type for the site from: a) OC Sands b) Aged NC Sands c) Recent NC Sands Each sand type has a family of curves that depend on mean normal stress. The program calculates mean normal stress and linearly interpolates between the two extremes provided in Baldi's chart.	Mean normal stress is evaluated from: $\sigma_m' = \frac{1}{3} \bullet (\sigma_v' + \sigma_h' + \sigma_h')^3$ where σ_v'= vertical effective stress σ_h'= horizontal effective stress and $\sigma_h = K_o * \sigma_v'$ with Ko assumed to be 0.5	5
q_{c1}	q_t normalized for overburden stress used for seismic analysis	$q_{c1} = q_t \bullet (Pa/\sigma_v')^{0.5}$ where: Pa = atm. Pressure q_t is in Mpa	3
q_{c1n}	q_{c1} in dimensionless form used for seismic analysis	$q_{c1n} = (q_{c1} / Pa)(Pa/\sigma_v')$ where: Pa = atm. Pressure and n ranges from 0.5 to 0.75 based on Ic.	3
K_{SPT}	Equivalent clean sand factor for $(N_1)60$	$K_{SPT} = 1 + ((0.75/30) * (FC - 5))$	10
K_{CPT}	Equivalent clean sand correction for q_{c1N}	$K_{cpt} = 1.0$ for $I_c \leq 1.64$ $K_{cpt} = f(I_c)$ for $I_c > 1.64$ (see reference)	10
q_{c1ncs}	Clean sand equivalent q_{c1n}	$q_{c1ncs} = q_{c1n} \bullet K_{cpt}$	3
CRR	Cyclic Resistance Ratio (for Magnitude 7.5)	$q_{c1ncs} < 50$: $CRR_{7.5} = 0.833 [(q_{c1ncs}/1000] + 0.05$ $50 \leq q_{c1ncs} < 160$: $CRR_{7.5} = 93 [(q_{c1ncs}/1000]^3 + 0.08$	10
CSR	Cyclic Stress Ratio	$CSR = (\tau_{av}/\sigma_v') = 0.65 (a_{max} / g) (\sigma_v/ \sigma_v') r_d$ $r_d = 1.0 - 0.00765$ z z $\leq$ 9.15m $r_d = 1.174 - 0.0267$ z 9.15 < z $\leq$ 23m $r_d = 0.744 - 0.008$ z 23 < z $\leq$ 30m $r_d = 0.50$ z > 30m	10

Interpreted Parameter	Description	Equation	Ref
MSF	Magnitude Scaling Factor	See Reference	10
FofS	Factor of Safety against Liquefaction	FS = ($CRR_{7.5}$ / CSR) MSF	10
Liquefaction Status	Statement indicating possible liquefaction	Takes into account FofS and limitations based I_c and q_{c1ncs}.	10

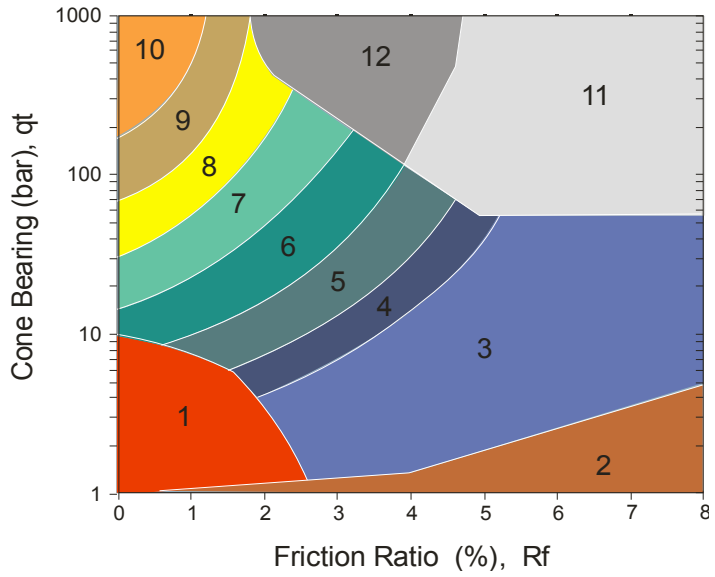

Zone	qt / N	Soil Behavior Type
1	2	sensitive fine grained
2	1	organic material
3	1	clay
4	1.5	silty clay to clay
5	2	clayey silt to silty clay
6	2.5	sandy silt to clayey silt
7	3	silty sand to sandy silt
8	4	sand to silty sand
9	5	sand
10	6	gravelly sand to sand
11	1	very stiff fine grained *
12	2	sand to clayey sand *

* overconsolidated or cemented

Figure 1 Non-Normalized Behavior Type Classification Chart

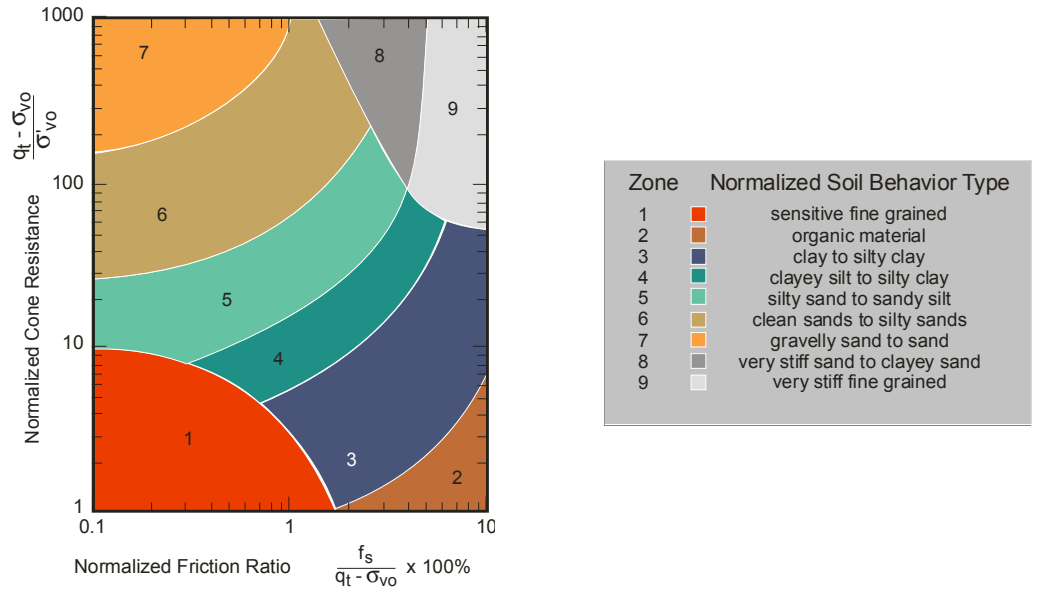

Figure 2 Normalized Behavior Type Classification Chart

Table 2 References

No.	References
1	Robertson, P.K., Campanella, R.G., Gillespie, D. and Greig, J., 1986, "Use of Piezometer Cone Data", Proceedings of InSitu 86, ASCE Specialty Conference, Blacksburg, Virginia.
2	Robertson, P.K., 1990, "Soil Classification Using the Cone Penetration Test", Canadian Geotechnical Journal, Volume 27.
3	Robertson, P.K. and Fear, C.E., 1998, "Evaluating cyclic liquefaction potential using the cone penetration test", Canadian Geotechnical Journal, 35: 442-459.
4	Robertson, P.K. and Wride, C.E., 1998, "Cyclic Liquefaction and its Evaluation Based on SPT and CPT", NCEER Workshop Paper, January 22, 1997
5	Lunne, T., Robertson, P.K. and Powell, J. J. M., 1997, " Cone Penetration Testing in Geotechnical Practice," Blackie Academic and Professional.
6	Plewes, H.D., Davies, M.P. and Jefferies, M.G., 1992, "CPT Based Screening Procedure for Evaluating Liquefaction Susceptibility", 45th Canadian Geotechnical Conference, Toronto, Ontario, October 1992.
7	Jefferies, M.G. and Davies, M.P., 1993. "Use of CPTu to Estimate equivalent N_{60}", Geotechnical Testing Journal, 16(4): 458-467.
8	Been, K. and Jefferies, M.P., 1985, "A state parameter for sands", Geotechnique, 35(2), 99-112.
9	Schmertmann, 1977, "Guidelines for Cone Penetration Test Performance and Design", Federal Highway Administration Report FHWA-TS-78-209, U.S. Department of Transportation
10	Proceedings of theNCEER Workshop on Evaluation of Liquefaction Resistance of Soils, Salt LakeCity, 1996. Chaired by Leslie Youd.

APPENDIX G
BOREHOLE GEOPHYSICS

- Borehole Geophysics Report

BOREHOLE GEOPHYSICS REPORT

Borehole Geophysical Logging
GEOVision, Inc.
November 14, 2006

GEOVision
geophysical services

FINAL REPORT

BORING GEOPHYSICAL LOGGING
BORINGS B-301, B-304, B-307, B-318
B-323, B-401, B-404, B-407, B-418 AND B-423

CALVERT CLIFFS NUCLEAR POWER PLANT
COMBINED OPERATING LICENSE APPLICATION
CALVERT COUNTY, MARYLAND

Report 6165-01 vol 1 of 2 rev A

November 14, 2006

FINAL REPORT

BORING GEOPHYSICAL LOGGING
BORINGS B-301, B-304, B-307, B-318
B-323, B-401, B-404, B-407, B-418 AND B-423

CALVERT CLIFFS NUCLEAR POWER PLANT
COMBINED OPERATING LICENSE APPLICATION
CALVERT COUNTY, MARYLAND

Report 6165-01 vol 1 of 2 rev A

November 14, 2006

Prepared for:

Schnabel Engineering, Inc.

Prepared by

GEOVision Geophysical Services
1151 Pomona Road, Unit P
Corona, California 92882
(951) 549-1234

TABLE OF CONTENTS

Table of Figures

Table of Tables

APPENDICIES

INTRODUCTION

Boring geophysical measurements were collected in ten uncased borings located at the Calvert Cliffs Nuclear Power Plant, located in Calvert County, Maryland. Geophysical data acquisition was performed between June 1 and June 30, 2006 by Rob Steller of **GEO***Vision*. The work was performed under subcontract with Schnabel Engineering, Inc., (Schnabel) with Brian Banks serving as the point of contact for Schnabel.

This report describes the field measurements, data analysis, and results of this work.

SCOPE OF WORK

This report presents the results of boring geophysical measurements collected between June 1 and June 30, 2006, in ten uncased borings, as detailed below. The purpose of these studies was to supplement stratigraphic information obtained during Schnabel's soil sampling program and to acquire shear wave velocities and compressional wave velocities as a function of depth, as a component of the Calvert Cliffs Nuclear Power Plant (CCNPP) Combined Operating License Application (COLA) Project.

BORING DESIGNATION	DATES LOGGED	ELEVATION	COORDINATES - FEET MARYLAND STATE PLANE (NAD 1927)	
			NORTH	EAST
B-301	6/5/06	96.84	217024.06	960815.05
B-304	6/1-2/06	68.00	217188.61	960896.88
B-307	6/15/06	119.28	216955.27	960690.13
B-318	6/4/06	NA	217019.30	961227.20
B-323	6/13/06	107.48	217027.97	960060.86
B-401	6/28/06	72.06	216344.12	961516.81
B-404	6/27/06	67.90	216441.34	961596.49
B-407	6/16/06	81.63	216238.96	961412.45
B-418	6/29-30/06	NA	216355.30	961988.60
B-423	6/13/06	110.14	216331.76	960850.21

Table 1 Boring locations and logging dates

The OYO/Robertson Model 3403 suspension logging telemetry unit, and the OYO Model 170 Suspension Logging Recorder and Suspension Logging Probe were used to obtain in-situ horizontal shear and compressional wave velocity measurements at 1.6 foot intervals. The acquired data was analyzed and a profile of velocity versus depth was produced for both compressional and horizontally polarized shear waves.

A detailed reference for the velocity measurement techniques used in this study is:

> Guidelines for Determining Design Basis Ground Motions, Report TR-102293, Electric Power Research Institute, Palo Alto, California, November 1993, Sections 7 and 8.

INSTRUMENTATION

Suspension Instrumentation

Suspension soil velocity measurements were performed in all borings using the Model 3403 suspension logging system, serial number 160023, manufactured by the Robertson Geologging division of OYO Corporation. Additional velocity measurements were performed in boring B-304 using the Model 170 suspension logging system, serial number 19029, manufactured by OYO Corporation. These additional measurements were made at the request of the client, to demonstrate that both systems produce the same results, and provide validation of each system. Both of these systems directly determines the average velocity of a 3.3 foot high segment of the soil column surrounding the boring of interest by measuring the elapsed time between arrivals of a wave propagating upward through the soil column. The receivers that detect the wave, and the source that generates the wave, are moved as a unit in the boring producing relatively constant amplitude signals at all depths.

Winch Geovision 4-conductor
Sheave - Measuring wheel Geovision S/N 102
OYO/Robertson Suspension telemetry unit Model 3403 S/N 160023
Or OYO PS170 Recorder and case Model 3331A S/N 19029
OYO PS Logger Borehole Probe, includes:
Reducer Model 3348A S/N 28063
Isolation tube, 1m Model 3387B S/N 28068
Weight Model 3302W S/N 12007
OYO PS 170 Source Model 3304 S/N 19043
Receiver/Sensor S/N 20040, S/N 30086
Driver Model 3386A S/N 27073

The suspension system probe consists of a combined reversible polarity solenoid horizontal shear-wave source (S_H) and compressional-wave source (P), joined to two biaxial receivers by a flexible isolation cylinder, as shown in Figure 1. The separation of the two receivers is 3.3 feet, allowing average wave velocity in the region between the receivers to be determined by inversion of the wave travel time between the two receivers. The total length of the probe as used in these surveys is 19 feet, with the center point of the receiver pair 12.1 feet above the bottom end of the probe.

The probe receives control signals from, and sends the amplified receiver signals to, instrumentation on the surface via an armored 4 conductor cable. The cable is wound onto the drum of a winch and is used to support the probe. Cable travel is measured to provide probe depth data, using a 3.28 foot circumference sheave fitted with a digital rotary encoder.

The entire probe is suspended in the boring by the cable, therefore, source motion is not coupled directly to the boring walls; rather, the source motion creates a horizontally propagating impulsive pressure wave in the fluid filling the boring and surrounding the source. This pressure wave is converted to P and S_H-waves in the surrounding soil and rock as it passes through the casing and grout annulus and impinges upon the wall of the boring. These waves propagate through the soil and rock surrounding the boring, in turn causing a pressure wave to be generated in the fluid surrounding the receivers as the soil waves pass their location. Separation of the P and S_H-waves at the receivers is performed using the following steps:

1. Orientation of the horizontal receivers is maintained parallel to the axis of the source, maximizing the amplitude of the recorded S_H -wave signals.
2. At each depth, S_H-wave signals are recorded with the source actuated in opposite directions, producing S_H-wave signals of opposite polarity, providing a characteristic S_H-wave signature distinct from the P-wave signal.
3. The 6.52 foot separation of source and receiver 1 permits the P-wave signal to pass and damp significantly before the slower S_H-wave signal arrives at the receiver. In faster soils or rock, the isolation cylinder is extended to allow greater separation of the P- and S_H-wave signals.

4. In saturated soils, the received P-wave signal is typically of much higher frequency than the received S_H-wave signal, permitting additional separation of the two signals by low pass filtering.
5. Direct arrival of the original pressure pulse in the fluid is not detected at the receivers because the wavelength of the pressure pulse in fluid is significantly greater than the dimension of the fluid annulus surrounding the probe (meter versus centimeter scale), preventing significant energy transmission through the fluid medium.

In operation, a distinct, repeatable pattern of impulses is generated at each depth as follows:

1. The source is fired in one direction producing dominantly horizontal shear with some vertical compression, and the signals from the horizontal receivers situated parallel to the axis of motion of the source are recorded.
2. The source is fired again in the opposite direction and the horizontal receiver signals are recorded.
3. The source is fired again and the vertical receiver signals are recorded. The repeated source pattern facilitates the picking of the P and S_H-wave arrivals; reversal of the source changes the polarity of the S_H-wave pattern but not the P-wave pattern.

The data from each receiver during each source activation is recorded as a different channel on the recording system. The Suspension PS system has six channels (two simultaneous recording channels), each with a 1024 sample record. The recorded data is displayed on a CRT or LCD display as six channels with a common time scale. Data is stored on disk for further processing. Up to 8 sampling sequences can be summed to improve the signal to noise ratio of the signals.

Review of the displayed data on the CRT, LCD or allows the operator to set the gains, filters, delay time, pulse length (energy), sample rate, and summing number to optimize the quality of the data before recording. Verification of the calibration of the Suspension PS digital recorder is performed every twelve months using a NIST traceable frequency source and counter, as outlined in Appendix C.

Caliper / Natural Gamma Instrumentation

Caliper and natural gamma data were collected using a Model 3ACS 3-leg caliper probe, serial numbers 2915 and 5368, manufactured by Robertson Geologging, Ltd. With the short arm configuration used in these surveys, the probes permitted measurement of boring diameters between 1.6 and 16 inches. With serial number 2915, caliper measurements were collected concurrent with measurement of natural gamma emission from the boring walls. Both probes were 6.82 feet long, and 1.5 inches in diameter.

This probe is useful in the following studies:

- Measurement of boring diameter and volume
- Location of hard and soft formations
- Location of fissures, caving, pinching and casing damage
- Bed boundary identification
- Strata correlation between borings

The probe receives control signals from, and sends the digitized measurement values to, a Robertson Micrologger II, S/N 5310, on the surface via an armored 4 conductor cable. The cable is wound onto the drum of a winch and is used to support the probe. Cable travel is measured to provide probe depth data, using a 3.28 foot circumference sheave fitted with a digital rotary encoder. The probe and depth data are transmitted by USB link from the Micrologger unit to a laptop computer where it is displayed and stored on hard disk.

The caliper consists of three arms, each with a toothed quadrant at their base, pivoted in the lower probe body. A toothed rack engages with each quadrant, thus constraining the arms to move together. Linear movement of the rack is converted to opening and closing of the arms. Springs hold the arms open in the operating position. A motor drive is provided to retract the arms, allowing the probe to be lowered into the boring. The rack is coupled to a potentiometer which converts movement into a voltage sensed by the probe's microprocessor.

Natural gamma measurements rely upon small quantities of radioactive material contained in all rocks to emit gamma radiation as they decay. Trace amounts of Uranium and Thorium are present in a few minerals, where potassium-bearing minerals such as feldspar, mica and clays will include traces of a radioactive isotope of Potassium. These emit gamma radiation as they decay with an extremely long half-life. This radiation is detected by scintillation - the production of a tiny flash of light when gamma rays strike a crystal of sodium iodide. The light is converted into an electrical pulse by a photomultiplier tube. Pulses above a threshold value of 60 KeV are counted by the probe's microprocessor. The measurement is useful because the radioactive elements are concentrated in certain rock types e.g. clay or shales, and depleted in others e.g. sandstone or coal.

Resistivity / Spontaneous Potential / Natural Gamma Instrumentation

Resistivity, spontaneous potential and natural gamma data were collected using a Model ELXG electric log probe, S/N 5490, manufactured by Robertson Geologging, Ltd. This probe measures Single Point Resistance (SPR), short normal (16") resistivity, long normal (64") resistivity, Spontaneous Potential (SP) and natural gamma. The probe is 8.20 feet long, and 1.73 inches in diameter.

This probe is useful in the following studies:

- Bed boundary identification
- Strata correlation between borings
- Strata geometry and type (shale indication)

The probe receives control signals from, and sends the digitized measurement values to, a Robertson Micrologger II, S/N 5310, on the surface via an armored 4 conductor cable. The cable is wound onto the drum of a winch and is used to support the probe. Cable travel is measured to provide probe depth data, using a 3.28 foot circumference sheave fitted with a digital rotary encoder. The probe and depth data are transmitted by USB link from the Micrologger unit to a laptop computer where it is displayed and stored on hard disk.

The resistivity section of the probe operates by driving an alternating current into the formation from the central SPR/DRIVE electrode. The current returns via the logging cable armor. To ensure adequate penetration of the formation the logging cable is insulated for approximately 30 feet from the cablehead. Voltages are measured between the 16" and 64" electrodes and the remote earth connection at surface, as noted below:

- Single Point Resistance (SPR): The current flowing to the cable armor is measured along with the voltage at the SPR electrode. The voltage divided by current gives resistance.

- Spontaneous Potential (SP): This is the DC bias of the 16" electrode with respect to the voltage return at the surface (ground stake).

Data quality depends upon good grounding at the surface. This is achieved with a metal stake driven into the mud-pit.

Natural gamma data was collected during the caliper data run.

Boring Deviation Instrumentation

Robertson Geologging HIRAT

Boring deviation data were collected in borings B-301, B-304, B-318, B-401, B-404 and B-418 using a High Resolution Acoustic Televiewer probe (HiRAT), serial numbers 5174 and 5500, manufactured by Robertson Geologging, Ltd. This probe is generally used to acquire acoustic images of the boring wall, but may also be used to collect boring deviation data. The probe is 7.58 feet long, and 1.9 inches in diameter, and is fitted with upper and lower four-arm centralizers.

In this application, this probe is useful in the following studies:

- Measurement of boring inclination and deviation from vertical
- Determination of need to correct soil and geophysical log depths to true vertical depths

The probe receives control signals from, and sends the digitized measurement values to, a Robertson Micrologger II, S/N 5310, on the surface via an armored 4 conductor cable. The cable is wound onto the drum of a winch and is used to support the probe. Cable travel is measured to provide probe depth data, using a 3.28 foot circumference sheave fitted with a digital rotary encoder. The probe and depth data are transmitted by USB link from the Micrologger unit to a laptop computer where it is displayed and stored on hard disk.

Mt. Sopris Deviation Probe

Boring deviation data were collected in borings B-307, B-323, B-407 and B-423 using a Model 2DVA-1000 deviation probe, manufactured by Mt. Sopris Instruments, Inc. The probe is 4.95 feet long, and 1.5 inches in diameter.

This probe is useful in the following studies:

- Measurement of boring inclination and deviation from vertical
- Determination of need to correct soil and geophysical log depths to true vertical depths

The probe receives control signals from, and sends the digitized measurement values to, a Mt. Sopris MGX II control unit, on the surface via an armored single conductor cable. The cable is wound onto the drum of a winch and is used to support the probe in the boring. Cable travel is measured to provide probe depth data, using a 0.5 foot circumference sheave fitted with a digital rotary encoder. The probe and depth data are transmitted by RS-232 serial link from the MGX II unit to a laptop computer where it is displayed and stored on hard disk.

MEASUREMENT PROCEDURES

Suspension Measurement Procedures

All ten borings were logged as uncased borings, filled with bentonite or polymer based drilling mud. Measurements followed the **GEO***Vision* Procedure for P-S Suspension Seismic Velocity Logging, revision 1.3, as presented in Appendix E. These procedures were supplied and approved in advance of the work. In each boring, the probe was positioned with the top of the probe at the top of the mud box, and the electronic depth counter was set to 8.2 feet, the distance between the mid-point of the receiver and the top of the probe, minus the height of the mud box, as verified with a tape measure, and recorded on the field logs. The probe was lowered to the bottom of the boring, and then returned to the surface, stopping at 1.6 foot intervals to collect data, as summarized in Table 2, below.

At each measurement depth the measurement sequence of two opposite horizontal records and one vertical record was performed, and the gains were adjusted as required. The data from each depth was printed on paper tape, checked, and recorded on diskette before moving to the next depth.

Upon completion of the measurements, the probe zero depth indication at the depth reference point was verified prior to removal from the boring.

Caliper / Natural Gamma Measurement Procedures

All ten borings were logged as uncased borings, filled with bentonite or polymer based drilling mud. Measurements followed the ASTM D6167 Conducting Borehole Geophysical Logging – Mechanical Caliper, as presented in Appendix E.

Prior to and following each logging run, the caliper tool was verified, using the manufacturer's supplied three point calibration jig, which is a circular plate with a series of holes in the top surface into which the tips of the caliper arms fit. This has circles of diameters from 2" to 12", with NIST

traceable calibration as documented in Appendix C. The calibration jig is placed over a bucket with the probe standing upright with its nose section passing through the jig's central hole. The caliper probe arms are opened under program control, and a log is recorded as the tips of the arms are placed in the holes on the calibration jig. The measured dimensions, as displayed on the recording computer screen was recorded on the field log sheet, as well as in the digital record, and compared with the calibration jig dimensions. If the verification records did not fall within +/- 0.05 inches of the calibration jig values, the caliper tool was re-calibrated, using the three point calibration jig, and the log repeated. As with the verification, the tips of the caliper arms are placed in the holes marked with the required diameter. During calibration, the value of the current calibration point, as stamped on the jig, is entered via the control computer. The system counts for 15 seconds to make an average of the response. The procedure is repeated for the second and third required openings.

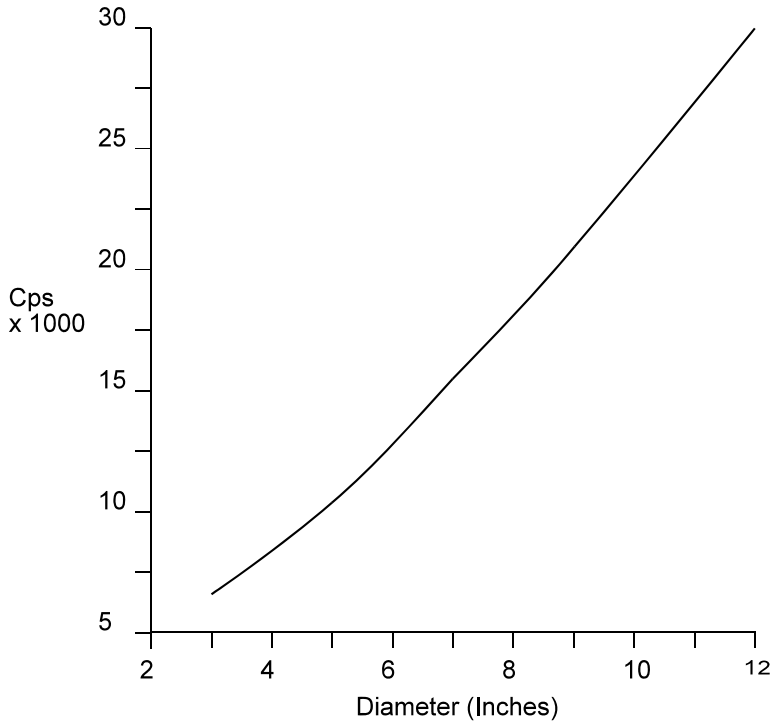

Figure 1. Example Calibration Curve for Caliper Probe

The computation and generation of the calibration coefficient file is entirely automatic. The calibration file is simply the set of coefficients of a quadratic curve which fits the three data points. Figure 1 shows the response of a caliper probe using data gathered during calibration.

Natural gamma was not calibrated in the field, as it is a qualitative measurement, not a quantitative value, and is used only to assist in picking transitions between stratigraphic units, as described in ASTM D6274, Conducting Borehole Geophysical Logging - Gamma, which is included in Appendix E.

In each boring, the probe was positioned with the top of the probe at the top of the mud box, and the electronic depth counter was set to 6.82 feet, the specified length of the probe, minus the height of the mud box, as verified with a tape measure, and recorded on the field logs. The probe was lowered to the bottom of the boring, where the caliper legs were opened, and data collection begun. The probe was then returned to the surface at 9.8 feet/sec, collecting data continuously at 0.05 foot spacing, as summarized in Table 2.

Upon completion of the measurements, the probe zero depth indication at the depth reference point was verified prior to removal from the boring, as summarized in Table 3.

Resistivity / Spontaneous Potential Measurement Procedures

All ten borings were logged as uncased borings, filled with bentonite or polymer based drilling mud. The probe was connected to the logging cable using a 32.8 foot long insulating cable section or “yoke”. The probe head was insulated by wrapping all exposed metal of the cablehead and probe with self-amalgamating insulation tape. The 32.8 foot insulating yoke was checked for any damage, and repaired with self-amalgamating insulation tape as needed.

The reference ground stake was driven firmly into the mud pit, and connected to the ground socket on the winch switch box.

This sonde was not calibrated in the field, as it is used to provide qualitative measurements, not quantitative values, and is used only to assist in picking transitions between stratigraphic units, as described in ASTM D5753, Planning and Conducting Borehole Geophysical Surveys, which is included in Appendix E.

In each boring, the probe was positioned with the top of the probe at the top of the mud box, and the electronic depth counter was set to 8.2 feet, the specified length of the probe, minus the height of the mud box, as verified with a tape measure. When logging on the smaller drill rigs, the depth was zeroed to the top of the yoke, and 32.8 feet was added to the zero depth, as recorded in the field logs. The probe was lowered to the bottom of the boring, where data collection was begun. The probe was then returned to the surface at 10 feet/sec, collecting data continuously at 0.05 foot spacing, as summarized in Table 2. The natural gamma data collected in these logs is redundant with the data collected in the caliper / natural gamma logs, and the caliper / natural data may be used to verify the natural gamma data collected in these logs.

Normally, when the un-insulated section of the logging cable leaves the boring fluid, the log is terminated, as the electrical measurements do not function under these conditions. However, in these surveys, the log was continued, in order to collect as much natural gamma data as possible before the yoke connector reached the measuring wheel.

Upon completion of the measurements, the probe zero depth indication at the depth reference point was verified prior to removal from the boring, as summarized in Table 3.

Boring Deviation Measurement Procedures

All ten borings were logged as uncased borings, filled with bentonite or polymer based drilling mud. Measurements followed the **GEO***Vision* standard field procedures, as presented in Appendix E.

Prior to use, the HiRAT or deviation probe tiltmeter and compass functions were checked by hanging from the drill rig and by comparison with a Brunton surveyors' compass.

In each boring logged with the Robertson HiRAT, the probe was positioned with the top of the probe at the top of the mud box, and the electronic depth counter was set to 4.71 feet, the specified length of the probe, minus the height of the mud box, as verified with a tape measure, and recorded on the field logs. In each boring logged with the Mt. Sopris 2DVA-1000, the probe was positioned with the bottom of the probe at the top of the mud box, and the electronic depth counter was set to 0.0 feet, minus the mud box height, as recorded on the field logs. The probe was lowered to the bottom of the boring, and data collection begun. The probe was then returned to the surface at 9.8 feet/sec, collecting data continuously, as summarized in Table 2.

Upon completion of the measurements, the probe zero depth indication at the depth reference point was verified prior to removal from the boring, as summarized in Table 3.

BORING NUMBER	TOOL AND RUN NUMBER	DEPTH RANGE (FEET)	OPEN HOLE (FEET)	DEPTH TO BOTTOM OF CASING (FEET)	SAMPLE INTERVAL (FEET)	DATE LOGGED
B-301	SUSPENSION 1	0.6 – 390.4	403.2	NO CASING	1.6	6/5/06
B-301	DEVIATION 1	0 – 402.5	-	NO CASING	.008	6/5/06
B-301	ELOG/GAMMA 1	402.0 – 1.7	-	NO CASING	0.05	6/5/06
B-301	ELOG/GAMMA 2	402.0 – 1.7	-	NO CASING	0.05	6/5/06
B-301	CALIPER 1	402.0 - 0	-	NO CASING	0.05	6/5/06
B-304	SUSPENSION 1	1.6 – 182.1	194.2	NO CASING	1.6	6/1/06
B-304	SUSPENSION 2	1.6 – 180.5	193.9	NO CASING	1.6	6/1/06
B-304	DEVIATION 1	0 – 194.0		NO CASING	.008	6/1/06
B-304	ELOG/GAMMA 1	40.5 – 195.4	195.4	NO CASING	0.05	6/1/06
B-304	ELOG/GAMMA 2	195.4 – 20.2	-	NO CASING	0.05	6/1/06
B-304	CALIPER 1	188.0 – 0	-	NO CASING	0.05	6/2/06
B-304	CALIPER 2	189.0 - 0	-	NO CASING	0.05	6/2/06
B-307	SUSPENSION 1	1.6 – 187.0	200.1	NO CASING	1.6	6/15/06
B-307	CALIPER 1	197.0 -0	-	NO CASING	0.05	6/15/06
B-307	ELOG 1	200.0 – 4.1	200	NO CASING	0.05	6/15/06
B-307	DEVIATION 1	0 – 195.0	-	NO CASING	0.1	6/15/06
B-318	SUSPENSION 1	1.6 – 190.3	203.0	NO CASING	1.6	6/4/06
B-318	DEVIATION 1	0 – 86.4	-	NO CASING	.008	6/4/06
B-318	DEVIATION 2	83.5 – 198.5	-	NO CASING	.008	6/4/06
B-318	ELOG/GAMMA 1	18.0 – 197.0	-	NO CASING	0.05	6/4/06
B-318	ELOG/GAMMA 2	197.0 – 40.0	-	NO CASING	0.05	6/4/06
B-318	CALIPER 1	195.0 - 0	-	NO CASING	0.05	6/4/06
B-323	SUSPENSION 1	1.6 – 190.3	203.4	NO CASING	1.6	6/4/06
B-323	CALIPER 1	203.5 - 0	-	NO CASING	0.05	6/4/06
B-323	ELOG/GAMMA 1	202.5 – 18.3	-	NO CASING	0.05	6/4/06
B-323	DEVIATION 1	190.0 – 180.0	-	NO CASING	0.1	6/4/06
B-323	DEVIATION 2	190.0 - 0	-	NO CASING	0.1	6/4/06
B-401	SUSPENSION 1	1.6 – 388.8	401.5	NO CASING	1.6	6/28/06
B-401	DEVIATION 1	3.2 – 401.0	-	NO CASING	.008	6/28/06
B-401	CALIPER/GAMMA 1	397.0 - 0	-	NO CASING	0.05	6/28/06
B-401	ELOG/GAMMA 1	399.5 – 1.8	-	NO CASING	0.05	6/28/06
B-404	SUSPENSION 1	1.6 – 187.0	199.8	NO CASING	1.6	6/27/06
B-404	DEVIATION 1	3.1 – 196.0	-	NO CASING	.008	6/27/06
B-404	CALIPER/GAMMA 1	195.0 - 0	-	NO CASING	0.05	6/27/06
B-404	ELOG/GAMMA 1	195.0 - 0	-	NO CASING	0.05	6/27/06
B-407	SUSPENSION 1	1.6 – 183.7	196.5	NO CASING	1.6	6/16/06
B-407	CALIPER 1	193.0 - 0	-	NO CASING	0.05	6/16/06
B-407	ELOG/GAMMA 1	197.0 – 17.6	197.0	NO CASING	0.05	6/16/06

B-407	DEVIATION 1	0 – 182.8	-	NO CASING	0.1	6/16/06
B-418	SUSPENSION 1	1.6 – 187.0	199.8	NO CASING	1.6	6/29/06
B-418	DEVIATION 1	199.4 – 3.3	199.4	NO CASING	.008	6/29/06
B-418	CALIPER/GAMMA 1	197.0 – 162.8	-	NO CASING	0.05	6/29/06
B-418	CALIPER/GAMMA 2	197.0 - 0	-	NO CASING	0.05	6/29/06
B-418	ELOG/GAMMA 1	197.0 20.0	-	NO CASING	0.05	6/29/06
B-423	DEVIATION 1	193.5 – 187.0	198.1	NO CASING	0.1	6/13/06
B-423	DEVIATION 2	193.5 - 0	-	NO CASING	0.1	6/13/06
B-423	SUSPENSION 1	1.6 – 185.4	-	NO CASING	1.6	6/13/06
B-423	CALIPER 1	193.0 – 0	-	NO CASING	0.05	6/13/06
B-423	ELOG/GAMMA 1	200.0 - 3.3	200.0	NO CASING	0.05	6/13/06

- PROBE DID NOT TOUCH BOTTOM OF BORING

Table 2. Logging dates and depth ranges

BORING NUMBER	TOOL AND RUN NUMBER	TOOL HIT BOTTOM DEPTH (FEET)	DRILLER DEPTH (FEET)	STARTING DEPTH REF. (FEET)	ENDING DEPTH REF. (FEET)	ASDE (FEET)
B-301	SUSPENSION 1	403.2	403	NA	NA	
B-301	DEVIATION 1	-	403	3.22	3.22	0.00
B-301	ELOG/GAMMA 1	-	403	6.70	6.70	0.00
B-301	ELOG/GAMMA 2	-	403	6.70	6.70	0.00
B-301	CALIPER 1	-	403	5.32	5.32	0.00
B-304	SUSPENSION 1	194.2	200	0.00	0.10	0.10
B-304	SUSPENSION 2	193.9	200	0.30	0.30	0.00
B-304	DEVIATION 1		200	3.22	3.22	0.00
B-304	ELOG/GAMMA 1	195.4	200	7.70	7.70	0.00
B-304	ELOG/GAMMA 2	-	200	7.70	7.70	0.00
B-304	CALIPER 1	-	200	5.32	5.32	0.00
B-304	CALIPER 2	-	200	5.32	5.32	0.00
B-307	SUSPENSION 1	200.1	200	6.64	6.64	0.00
B-307	CALIPER 1	-	200	5.32	5.32	0.00
B-307	ELOG 1	200	200	6.70	6.70	0.00
B-307	DEVIATION 1	-	200	-1.50	-1.50	0.00
B-318	SUSPENSION 1	203.0	201	NA	NA	
B-318	DEVIATION 1	-	201	3.22	3.22	0.00
B-318	DEVIATION 2	-	201	3.22	3.22	0.00
B-318	ELOG/GAMMA 1	-	201	39.95	39.95	0.00
B-318	ELOG/GAMMA 2	-	201	39.95	39.95	0.00
B-318	CALIPER 1	-	201	5.32	5.32	0.00
B-323	SUSPENSION 1	203.4	200	6.43	6.69	0.26
B-323	CALIPER 1	-	200	5.12	5.12	0.00
B-323	ELOG/GAMMA 1	-	200	39.50	39.50	0.00
B-323	DEVIATION 1	-	200	-1.50	-3.13	1.63
B-323	DEVIATION 2	-	200	-1.50	-1.50	0.00
B-401	SUSPENSION 1	401.5	400	6.63	6.69	0.06
B-401	DEVIATION 1	-	400	3.22	3.22	0.00
B-401	CALIPER/GAMMA 1	-	400	5.32	5.45	0.13
B-401	ELOG/GAMMA 1	-	400	6.70	6.75	0.05
B-404	SUSPENSION 1	199.8	200	0.00	0.00	0.00
B-404	DEVIATION 1	-	200	3.12	3.15	0.02
B-404	CALIPER/GAMMA 1	-	200	5.12	5.10	0.02
B-404	ELOG/GAMMA 1	-	200	39.40	39.45	0.05
B-407	SUSPENSION 1	196.5	200	NA	NA	
B-407	CALIPER 1	-	200	5.32	5.32	0.00

B-407	ELOG/GAMMA 1	197.0	200	39.50	39.50	0.00
B-407	DEVIATION 1	-	200	-1.50	-1.50	0.00
B-418	SUSPENSION 1	199.8	200	0.00	0.00	0.00
B-418	DEVIATION 1	199.4	200	3.22	3.25	0.02
B-418	CALIPER/GAMMA 1	-	200	5.32	5.35	0.03
B-418	CALIPER/GAMMA 2	-	200	5.32	5.32	0.00
B-418	ELOG/GAMMA 1	-	200	39.50	39.50	0.00
B-423	DEVIATION 1	198.1	200	-1.80	-3.10	1.30
B-423	DEVIATION 2	-	200	-1.80	-1.80	0.00
B-423	SUSPENSION 1	-	200	6.33	6.33	0.00
B-423	CALIPER 1	-	200	5.02	5.02	0.00
B-423	ELOG/GAMMA 1	200.0	200	6.40	6.40	0.00

- PROBE DID NOT TOUCH BOTTOM OF BORING

Table 3. Boring Bottom Depths and After Survey Depth Error (ASDE)

DATA ANALYSIS

Suspension Analysis

Using the proprietary OYO program PSLOG.EXE version 1.0, included in volume 2 of 2 (CDR) of this report, the recorded digital waveforms were analyzed to locate the most prominent first minima, first maxima, or first break on the vertical axis records, indicating the arrival of P-wave energy. The difference in travel time between receiver 1 and receiver 2 (R1-R2) arrivals was used to calculate the P-wave velocity for that 3.3 foot segment of the soil column. When observable, P-wave arrivals on the horizontal axis records were used to verify the velocities determined from the vertical axis data. The time picks were then transferred into an EXCEL template (EXCEL version 2003 SP2) to complete the velocity calculations based upon the arrival time picks made in PSLOG. The PSLOG pick files and the EXCEL analysis files are included in the boring specific directories on volume 2 of 2 (CDR) of this report.

The P-wave velocity over the 6.5 foot interval from source to receiver 1 (S-R1) was also picked using PSLOG, and calculated and plotted in EXCEL, for quality assurance of the velocity derived from the travel time between receivers. In this analysis, the depth values as recorded were

increased by 4.9 feet to correspond to the mid-point of the 6.5 foot S-R1 interval, as illustrated in Figure 1. Travel times were obtained by picking the first break of the P-wave signal at receiver 1 and subtracting 0.3 milliseconds, the calculated and experimentally verified delay from source trigger pulse (beginning of record) to source impact. This delay corresponds to the duration of acceleration of the solenoid before impact.

As with the P-wave records, using PSLOG, the recorded digital waveforms were analyzed to locate the presence of clear S_H-wave pulses, as indicated by the presence of opposite polarity pulses on each pair of horizontal records. Ideally, the S_H-wave signals from the 'normal' and 'reverse' source pulses are very nearly inverted images of each other. Digital FFT - IFFT lowpass filtering was used to remove the higher frequency P-wave signal from the S_H-wave signal. Different filter cutoffs were used to separate P- and S_H-waves at different depths, ranging from 600 Hz in the slowest zones to 2000 Hz in the regions of highest velocity. At each depth, the filter frequency was selected to be at least twice the fundamental frequency of the S_H-wave signal being filtered.

Generally, the first maxima were picked for the 'normal' signals and the first minima for the 'reverse' signals, although other points on the waveform were used if the first pulse was distorted. The absolute arrival time of the 'normal' and 'reverse' signals may vary by +/- 0.2 milliseconds, due to differences in the actuation time of the solenoid source caused by constant mechanical bias in the source or by boring inclination. This variation does not affect the R1-R2 velocity determinations, as the differential time is measured between arrivals of waves created by the same source actuation. The final velocity value is the average of the values obtained from the 'normal' and 'reverse' source actuations.

As with the P-wave data, S_H-wave velocity calculated from the travel time over the 6.5 foot interval from source to receiver 1 was calculated and plotted for verification of the velocity derived from the travel time between receivers. In this analysis, the depth values were increased by 4.9 foot to correspond to the mid-point of the 6.5 foot S-R1 interval. Travel times were obtained by picking the first break of the S_H-wave signal at the near receiver and subtracting 0.3 milliseconds, the calculated and experimentally verified delay from the beginning of the record at the source trigger pulse to source impact.

These data and analysis were reviewed by John Diehl and Tony Martin as a component of **GEO***Vision*'s in-house QA-QC program.

Figure 2 shows an example of R1 - R2 measurements on a sample filtered suspension record. In Figure 2, the time difference over the 3.3 foot interval of 1.88 milliseconds for the horizontal signals is equivalent to an S_H-wave velocity of 1745 feet/second. Whenever possible, time differences were determined from several phase points on the S_H-waveform records to verify the data obtained from the first arrival of the S_H-wave pulse. Figure 3 displays the same record before filtering of the S_H-waveform record with a 1400 Hz FFT - IFFT digital lowpass filter, illustrating the presence of higher frequency P-wave energy at the beginning of the record, and distortion of the lower frequency S_H-wave by residual P-wave signal.

Caliper / Natural Gamma Analysis

No analysis is required with the caliper or natural gamma data, however depths to identifiable boring features were compared to verify compatible depth readings on all logs. These data were combined with the resistivity, ELOG based natural gamma and spontaneous potential (SP) logs, and converted to LAS and PDF formats for transmittal to the client.

Resistivity / Natural Gamma / Spontaneous Potential Analysis

No analysis is required with the resistivity, natural gamma or spontaneous potential data, however depths to identifiable boring features were compared to verify compatible depth readings on all logs. These data were combined with the caliper and caliper-based natural gamma logs, and converted to LAS and PDF formats for transmittal to the client.

Boring Deviation Analysis

Robertson Geologging HIRAT

The collected Acoustic Televiewer data was processed with Robertson Geologging's RGLDIP program, version 6.2, to extract the deviation data and produce an ASCII file and plots of deviation data.

Mt. Sopris Deviation Probe

Deviation logs in borings B-307, B-323, B-407 and B-423 were surveyed using the Mt. Sopris 2DVA-100 probe, and the results were analyzed by Nate Davis of COLOG, using Mt. Sopris MSLOG 7.2 program to produce an ASCII file and plots of deviation data.

RESULTS

Suspension Results

Suspension R1-R2 P- and S_H-wave velocities are plotted in Figures 5, 8, 9, 12, 15, 18, 21, 24, 27, 30 and 33. The suspension velocity data presented in these figures are presented in Tables 5 - 15. The PSLOG and EXCEL analysis files for each boring are included in the boring specific directories on volume 2 of 2 (CDR) of this report, along with the raw and filtered waveforms.

P- and S_H-wave velocity data from R1-R2 analysis and quality assurance analysis of S-R1 data are plotted together in Figures A-1 through A-11 to aid in visual comparison. It must be noted that R1-R2 data is an average velocity over a 3.3 foot segment of the soil column; S-R1 data is an average over 6.5 feet, creating a significant smoothing relative to the R1-R2 plots. S-R1 data are presented in Tables A-1 through A-11, and included in the EXCEL analysis files for each boring on volume 2 of 2 (CDR) of this report.

Calibration procedures and records for the suspension measurement system are presented in Appendix C.

The **GEO***Vision* standard field log sheets for all borings are reproduced in Appendix D.

The **GEO***Vision* standard field procedures are reproduced in Appendix E.

Caliper/ Natural Gamma Results

Caliper and natural gamma data is presented in combined log plots with resistivity and spontaneous potential as single page logs in Figures 6, 10, 13, 16, 19, 22, 25, 28, 31 and 34, as well as multi-page logs in Appendix B. LAS 2.0 data and Acrobat files of the plots for each boring are included in the boring specific sub-directories in the data directory on volume 2 of 2 (CDR) of this report.

Resistivity / Spontaneous Potential Results

Resistivity and spontaneous potential data is presented in combined log plots with caliper and natural gamma data as single page logs in Figures 6, 10, 13, 16, 19, 22, 25, 28, 31 and 34, as well as multi-page logs in Appendix B. LAS 2.0 data and Acrobat files for each boring are included in the boring specific sub-directories in the data directory on volume 2 of 2 (CDR) of this report.

Boring Deviation Results

Boring deviation data is presented graphically in Figures 7, 11, 14, 17, 20, 23, 26, 29, 32 and 35, and summarized in Table 4. Deviation data plots in Acrobat format and deviation data at 1.0 foot stations are presented in text format in the boring specific sub-directories in the data directory on volume 2 of 2 (CDR) of this report.

SUMMARY

Discussion of Suspension Results

Suspension PS velocity data is ideally collected in an uncased fluid filled boring, drilled with rotary mud (rotary wash) methods. All of the borings at this site were ideal for collection of Suspension PS velocity data, with minor exceptions due to some significant wash-outs of the borings at water table, as shown in the caliper logs. Despite these washouts, the quality of these data ranged from good to excellent. Each boring is discussed in more detail below.

Suspension PS velocity data quality is judged based upon 5 criteria:

1. Consistent data between receiver to receiver (R1 – R2) and source to receiver (S – R1) data.
2. Consistent relationship between P-wave and S_H -wave (excluding transition to saturated soils)
3. Consistency between data from adjacent depth intervals.
4. Clarity of P-wave and S_H-wave onset, as well as damping of later oscillations.
5. Consistency of profile between adjacent borings, if available.

B-301: These data show excellent correlation between R1 – R2 and S – R1 data, as well as excellent correlation between P-wave and S_H-wave velocities. P-wave and S_H-wave onsets are generally clear, and later oscillations are well damped. This data set agrees well with data from other borings on the site, when depth shifted to correct for boring collar elevation. This is an excellent velocity data set.

B-304: These data show excellent correlation between R1 – R2 and S – R1 data, as well as excellent correlation between P-wave and S_H-wave velocities. P-wave and S_H-wave onsets are generally clear, and later oscillations are well damped. This data set agrees well with data from other borings on the site, when depth shifted to correct for boring collar elevation. This is an excellent velocity data set.

B-307: These data show excellent correlation between R1 – R2 and S – R1 data, as well as excellent correlation between P-wave and S_H-wave velocities. P-wave and S_H-wave onsets are generally clear, and later oscillations are well damped. This data set agrees well with data from other borings on the site, when depth shifted to correct for boring collar elevation. This is an excellent velocity data set.

B-318: These data show excellent correlation between R1 – R2 and S – R1 data, as well as excellent correlation between P-wave and S_H-wave velocities. P-wave and S_H-wave onsets are generally clear, and later oscillations are well damped. This data set agrees well with data from other borings on the site, when depth shifted to correct for boring collar elevation. This is an excellent velocity data set.

B-323: These data show excellent correlation between R1 – R2 and S – R1 data, as well as excellent correlation between P-wave and S_H-wave velocities. P-wave and S_H-wave onsets are generally clear, and later oscillations are well damped. This data set agrees well with data from other borings on the site, when depth shifted to correct for boring collar elevation. This is an excellent velocity data set.

B-401: These data show excellent correlation between R1 – R2 and S – R1 data, as well as excellent correlation between P-wave and S_H-wave velocities. P-wave and S_H-wave onsets are generally clear, and later oscillations are well damped. This data set agrees well with data from other borings on the site, when depth shifted to correct for boring collar elevation. This is an excellent velocity data set.

B-404: These data show excellent correlation between R1 – R2 and S – R1 data, as well as excellent correlation between P-wave and S_H-wave velocities. P-wave and S_H-wave onsets are generally clear, and later oscillations are well damped. This data set agrees well with data from other borings on the site, when depth shifted to correct for boring collar elevation. This is an excellent velocity data set.

B-407: These data show excellent correlation between R1 – R2 and S – R1 data, as well as excellent correlation between P-wave and S_H-wave velocities. P-wave and S_H-wave onsets are generally clear, and later oscillations are well damped. This data set agrees well with data from other borings on the site, when depth shifted to correct for boring collar elevation. This is an excellent velocity data set.

B-418: These data show excellent correlation between R1 – R2 and S – R1 data, as well as excellent correlation between P-wave and S_H-wave velocities. P-wave and S_H-wave onsets are generally clear, and later oscillations are well damped. This data set agrees well with data from other borings on the site, when depth shifted to correct for boring collar elevation. This is an excellent velocity data set.

B-423: These data show excellent correlation between R1 – R2 and S – R1 data, as well as excellent correlation between P-wave and S_H-wave velocities. P-wave and S_H-wave onsets are generally clear, and later oscillations are well damped. This data set agrees well with data from other borings on the site, when depth shifted to correct for boring collar elevation. This is an excellent velocity data set.

Discussion of Caliper / Natural Gamma Results

B-301: Caliper data shows erosion of the upper 30 feet of the boring, and several washouts to greater than 12 inches diameter. Below 42 feet, boring gauge is very consistent. Natural gamma was not collected with this tool in this boring.

B-304: Caliper data shows no erosion of the upper section of this boring. The boring gauge is very consistent for the entire depth. Natural gamma was not collected with this tool in this boring.

B-307: Caliper data shows erosion of the upper 20 feet of the boring, and several washouts to greater than 12 inches diameter. Below 20 feet, boring gauge is very consistent, with a small narrowing at approximately 165 feet. Natural gamma was not collected with this tool in this boring.

B-318: Caliper data shows slight erosion of the upper 45 feet of the boring, with several washouts to 7 inches diameter. Below 45 feet, the boring gauge is variable. Natural gamma was not collected with this tool in this boring.

B-323: Caliper data shows erosion of the upper 20 feet of the boring, and several washouts to greater than 12 inches diameter. Below 20 feet, boring gauge is very consistent, with a small narrowing at approximately 165 feet. Natural gamma was not collected with this tool in this boring.

B-401: Caliper data shows erosion of the upper 20 feet of the boring, and several washouts to greater than 12 inches diameter. Below 45 feet, boring gauge is very consistent. Natural gamma was collected with this tool in this boring, as well as with the ELOG tool, and the comparison between the two data sets provides an almost exact match, verifying the performance of the natural gamma measuring systems.

B-404: Caliper data shows erosion of the upper 45 feet of the boring, and a number of washouts to 8 - 12 inches diameter. Below 45 feet, boring gauge is consistent. Natural gamma was collected with this tool in this boring, as well as with the ELOG tool, and the comparison between the two data sets provides an almost exact match, verifying the performance of the natural gamma measuring systems.

B-407: Caliper data shows some erosion of the upper 55 feet of the boring, though this boring was drilled with a 5 inch bit to 55 feet, and the boring is close to this gauge. One washout to greater than 12 inches diameter occurs at approximately 7 feet. Below 55 feet, boring gauge is very consistent. Natural gamma was not collected with this tool in this boring.

B-418: Caliper data shows erosion of the upper 12 feet of the boring, and a several shallow washouts to 8 inches diameter. Below 12 feet, boring gauge is consistent, with periodic increases in diameter which correspond to bit location when flushing the boring before collecting a drive sample. Natural gamma was collected with this tool in this boring, as well as with the ELOG tool, and the comparison between the two data sets provides an almost exact match, verifying the performance of the natural gamma measuring systems.

B-423: Caliper data shows erosion of the upper 30 feet of the boring, and one large washout to greater than 12 inches diameter. Below 30 feet, boring gauge is consistent. Natural gamma was not collected with this tool in this boring.

.

Discussion of Resistivity / Spontaneous Potential Results

B-301: These data show good correlation between the different logs below 40 feet. The electrical data is degraded above this depth, as the upper yoke electrode moves out of the boring fluid at this depth. The natural gamma data remains good to the surface, and agrees well with data from other borings at this site, when depth shifted to correct for elevation differences.

B-304: These data show good correlation between the different logs below 40 feet. The electrical data is degraded above this depth, as the upper yoke electrode moves out of the boring fluid at this depth. The natural gamma data remains good to 20 feet, where the log was stopped as the upper yoke electrode had reached the top of the drill rig tower.

B-307: These data show good correlation between the different logs below 40 feet. The electrical data is degraded above this depth, as the upper yoke electrode moves out of the boring fluid at this depth. The natural gamma data remains good to 8 feet, where the log was stopped as the upper yoke electrode had reached the top of the drill rig tower.

B-318: These data show good correlation between the different logs below 40 feet. The electrical data is degraded above this depth, as the upper yoke electrode moves out of the boring fluid at this depth. The natural gamma data remains good to 20 feet, where the log was stopped as the upper yoke electrode had reached the top of the drill rig tower.

B-323: These data show good correlation between the different logs below 40 feet. The electrical data is degraded above this depth, as the upper yoke electrode moves out of the boring fluid at this depth. The natural gamma data remains good to 20 feet, where the log was stopped as the upper yoke electrode had reached the top of the drill rig tower.

B-401: These data show good correlation between the different logs below 40 feet. The electrical data is degraded above this depth, as the upper yoke electrode moves out of the boring fluid at this depth. The natural gamma data remains good to the surface, and agrees well with data from other borings at this site, when depth shifted to correct for elevation differences. Comparison between the two natural gamma data sets in this boring provides an almost exact match, verifying the performance of the natural gamma measuring systems.

B-404: These data show good correlation between the different logs below 40 feet. The electrical data is degraded above this depth, as the upper yoke electrode moves out of the boring fluid

at this depth. The natural gamma data remains good to the surface, and agrees well with data from other borings at this site, when depth shifted to correct for elevation differences. Comparison between the two natural gamma data sets in this boring provides an almost exact match, verifying the performance of the natural gamma measuring systems.

B-407: These data show good correlation between the different logs below 40 feet. The electrical data is degraded above this depth, as the upper yoke electrode moves out of the boring fluid at this depth. The natural gamma data remains good to 20 feet, where the log was stopped as the upper yoke electrode had reached the top of the drill rig tower.

B-418: These data show good correlation between the different logs below 40 feet. The electrical data is degraded above this depth, as the upper yoke electrode moves out of the boring fluid at this depth. The natural gamma data remains good to 20 feet and agrees well with data from other borings at this site, when depth shifted to correct for elevation differences. Comparison between the two natural gamma data sets in this boring provides an almost exact match, verifying the performance of the natural gamma measuring systems.

B-423: These data show good correlation between the different logs below 40 feet. The electrical data is degraded above this depth, as the upper yoke electrode moves out of the boring fluid at this depth. The natural gamma data remains good to the surface.

Discussion of Boring Deviation Results

All ten borings were inclined at less than 1 degree from vertical, and the maximum error in depth value was less than 0.1 foot, as presented in Table 4. This error is significantly less than depth errors from other causes, and no adjustment of log depths are indicated.

BORING NUMBER	MEAN DEVIATION AND AZIMUTH (DEGREES)	SURVEY DEPTH (FEET)	VERTICAL DEPTH (FEET)	DEPTH ERROR (FEET)	HORIZONTAL OFFSET (FEET)
B-301	0.52 - N167.9	403.0	403.0	0.0	3.69
B-304	0.69 – N249.6	194.3	194.3	0.0	2.32
B-307	0.76 – N256.4	195.2	195.2	0.0	2.58
B-318	0.74 – N147.2	198.5	198.4	0.1	2.58
B-323	0.38 – N256.4	189.9	189.9	0.0	1.26
B-401	0.91 – N264.8	401.3	401.2	0.1	6.38
B-404	0.28 – N189.5	196.8	196.8	0.0	0.95
B-407	0.61 – N271.2	182.8	182.7	0.1	1.99
B-418	0.32 – N187.9	199.3	199.3	0.0	1.12
B-423	0.42 – N76.6	193.5	193.5	0.0	1.41

Table 4. Boring Deviation Data Summary

Quality Assurance

These boring geophysical measurements were performed using industry-standard or better methods for measurements and analyses. All work was performed under **GEO***Vision* quality assurance procedures, which include:

- Use of NIST-traceable calibrations, where applicable, for field and laboratory instrumentation
- Use of standard field data logs
- Use of independent verification of velocity data by comparison of receiver-to-receiver and source-to-receiver velocities
- Independent review of calculations and results by a registered professional engineer, geologist, or geophysicist.

Suspension Data Reliability

P- and S_H-wave velocity measurement using the Suspension Method gives average velocities over a 3.3 foot interval of depth. This high resolution results in the scatter of values shown in the graphs. Individual measurements are very reliable with estimated precision of +/- 5%. Standardized field procedures and quality assurance checks contribute to the reliability of these data.

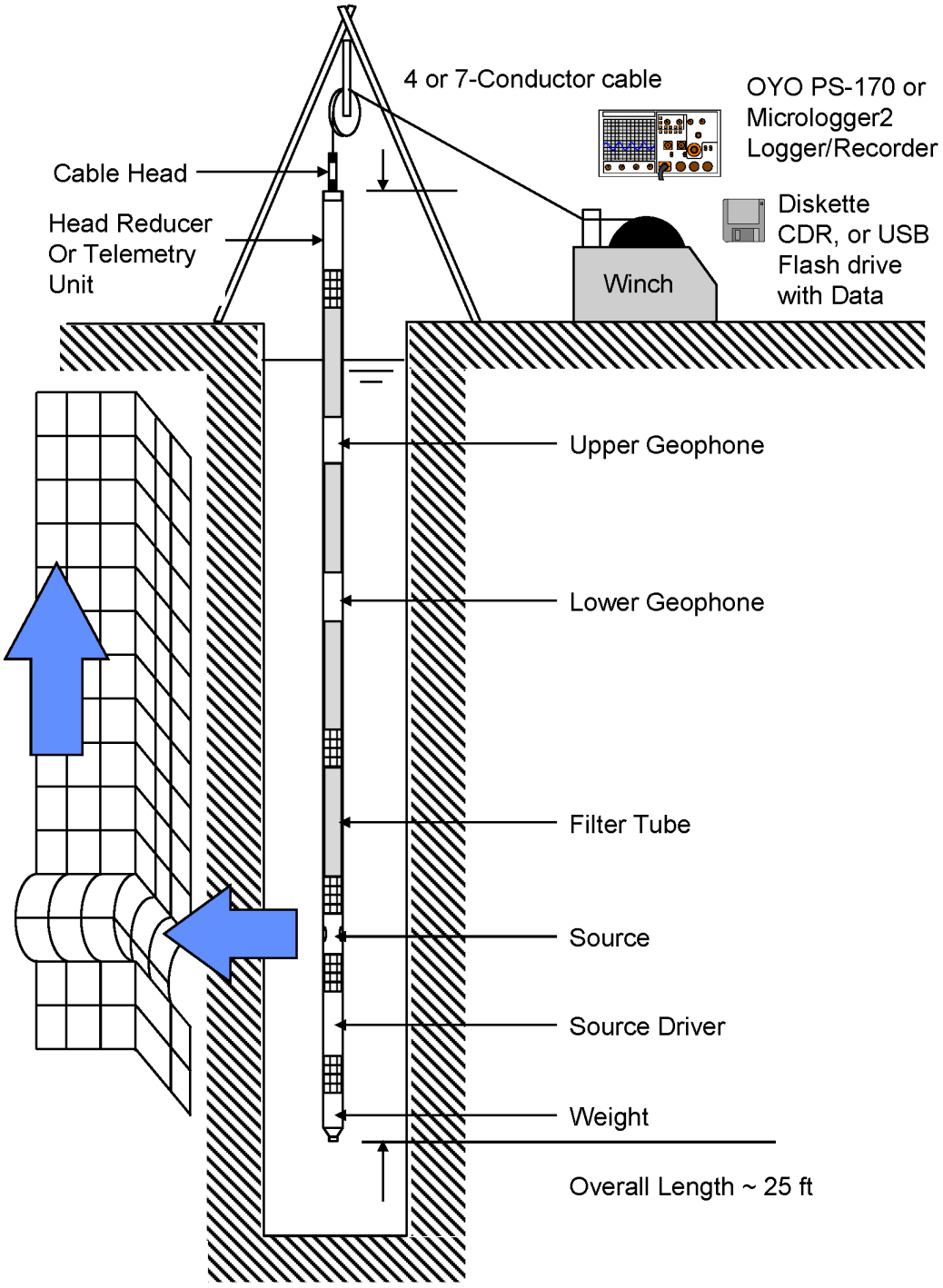

Figure 2: Concept illustration of P-S logging system

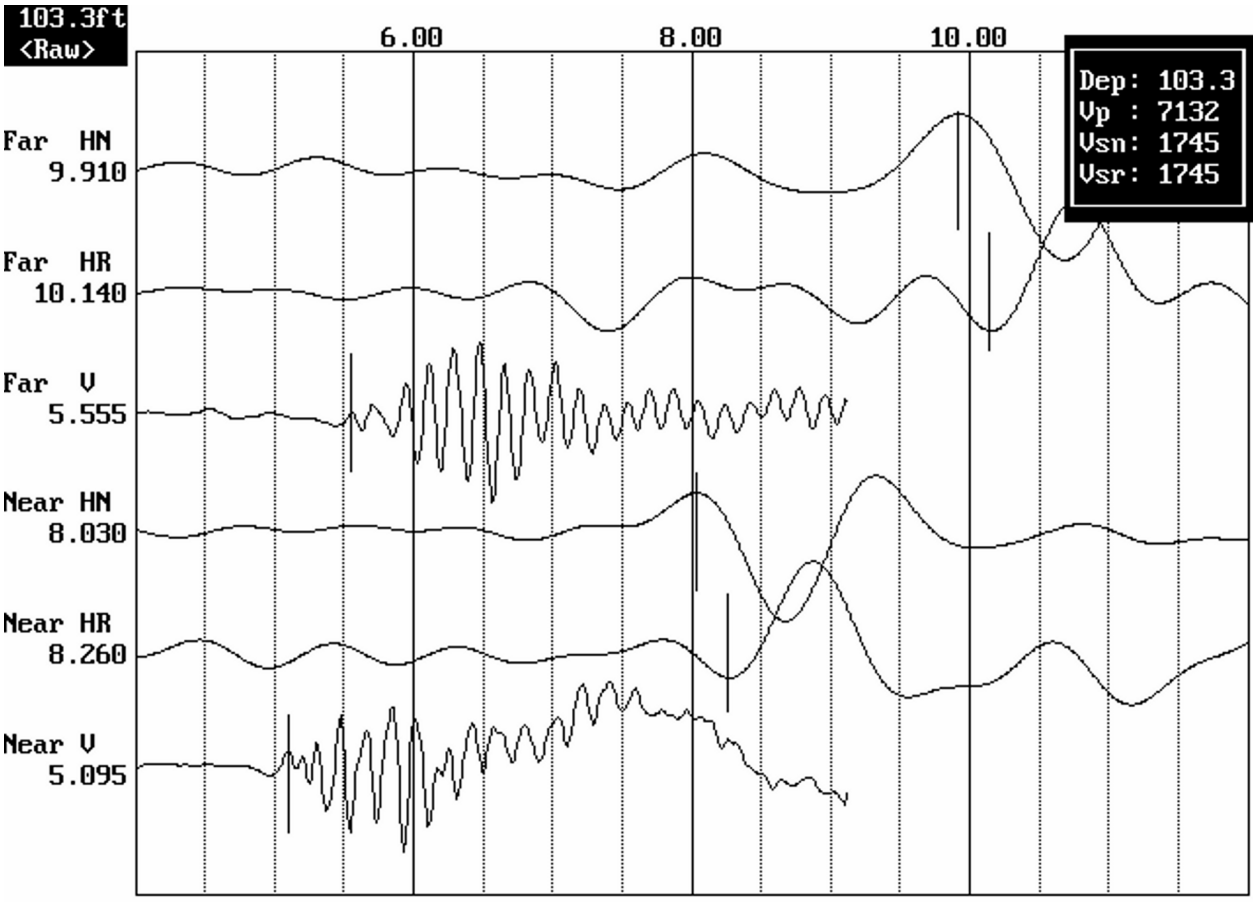

Figure 3: Example of filtered (1400 Hz lowpass) record

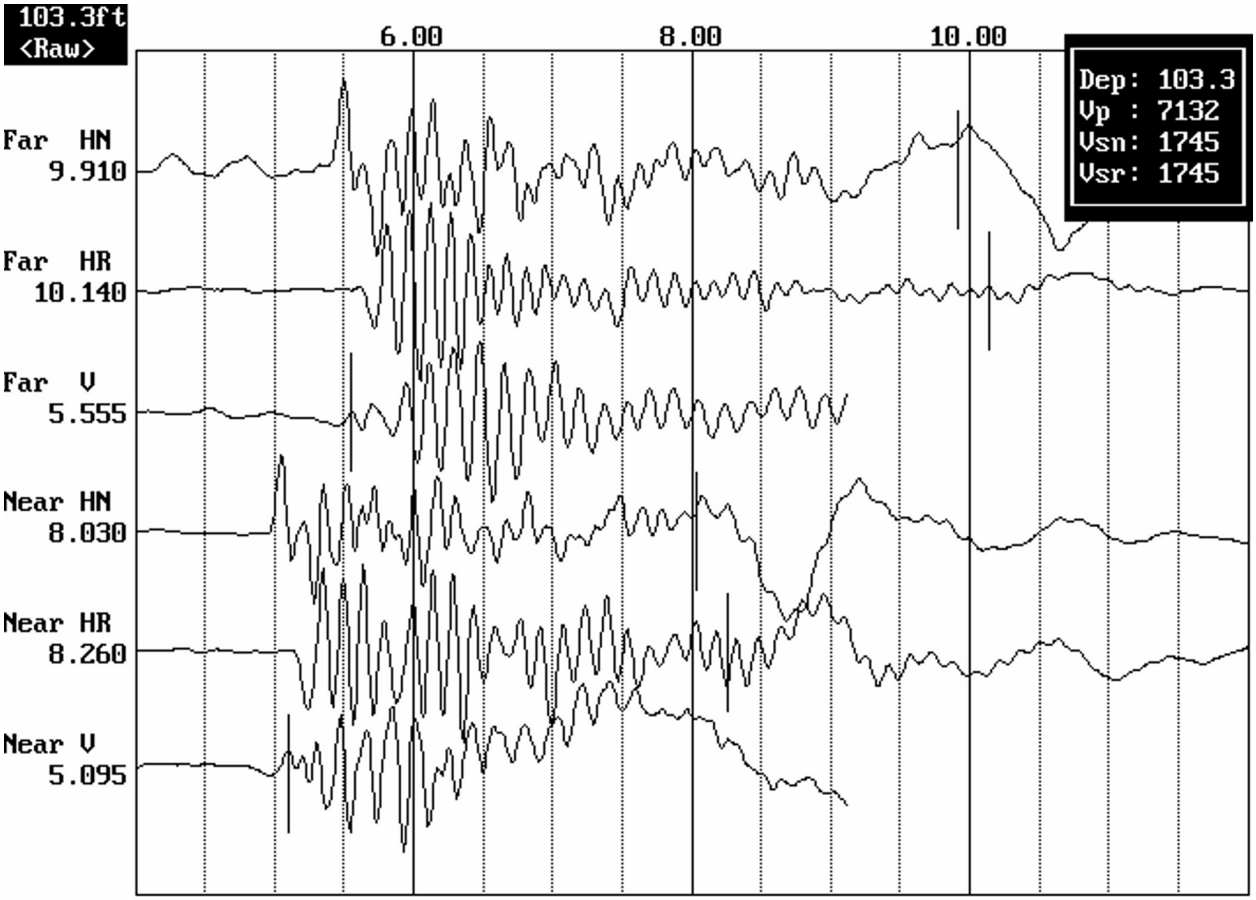

Figure 4. Example of unfiltered record

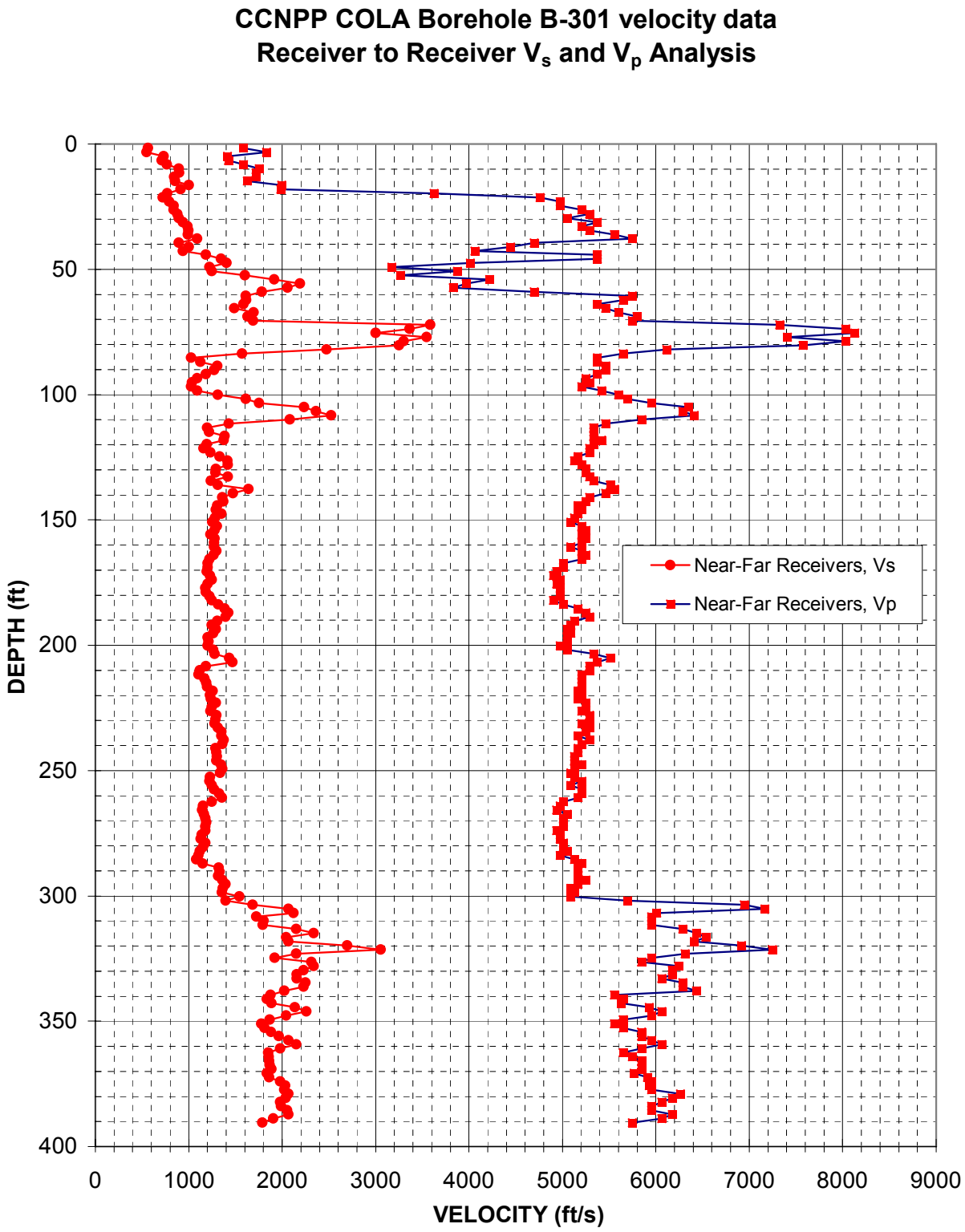

Figure 5: Boring B-301, Suspension R1-R2 P- and S_H-wave velocities

Depth (feet)	V_s (feet/sec)	V_p (feet/sec)
1.6	560	1590
3.3	550	1830
4.9	730	1410
6.6	710	1420
8.2	770	1590
9.8	890	1750
11.5	900	1720
13.1	840	1720
14.8	850	1630
16.4	1000	2000
18.0	920	1980
19.7	770	3620
21.3	720	4760
23.0	790	4980
24.6	840	4980
26.3	840	5210
27.9	880	5290
29.5	900	5050
31.2	940	5380
32.8	990	5210
34.5	1000	5290
36.1	990	5560
37.7	1090	5750
39.4	900	4690
41.0	1000	4440
42.7	940	4070
44.3	1180	5380
45.9	1340	5380
47.6	1410	4020
49.2	1220	3170
50.9	1250	3880
52.5	1600	3270
54.1	1920	4220
55.8	2190	3970
57.4	2060	3830
59.1	1780	4690
60.7	1610	5750
62.3	1620	5650
64.0	1590	5380
65.6	1490	5460
67.3	1700	5600
68.9	1630	5800
70.5	1690	5750
72.2	3580	7330
73.8	3370	8030
75.5	3000	8130
77.1	3550	7410
78.7	3300	8030
80.4	3250	7580
82.0	2480	6120
83.7	1570	5650
85.3	1030	5380
86.9	1130	5380
88.6	1310	5460
90.2	1270	5460
91.9	1190	5380
93.5	1090	5250
95.1	1040	5290
96.8	1030	5210
98.4	1090	5420
100.1	1310	5600
101.7	1610	5700
103.4	1750	5950
105.0	2240	6350
106.6	2360	6290
108.3	2530	6410
109.9	2080	5850
111.6	1430	5460
113.2	1200	5330
114.8	1220	5330
116.5	1380	5330
118.1	1380	5420
119.8	1190	5330
121.4	1160	5290
123.0	1230	5290
124.7	1330	5170
126.3	1410	5130
128.0	1420	5210
129.6	1290	5250
131.2	1290	5250
132.9	1420	5290
134.5	1240	5330
136.2	1310	5510
137.8	1640	5560
139.4	1470	5460
141.1	1360	5290
142.7	1370	5250
144.4	1310	5170
146.0	1290	5210
147.6	1350	5170
149.3	1280	5130
150.9	1250	5090
152.6	1300	5210
154.2	1280	5250
155.8	1230	5210
157.5	1280	5250
159.1	1270	5210
160.8	1270	5090
162.4	1300	5210
164.0	1270	5250
165.7	1220	5210
167.3	1200	5010
169.0	1200	5010
170.6	1190	4940
172.2	1230	4900
173.9	1250	4980
175.5	1200	4940
177.2	1180	4980
178.8	1190	4980
180.5	1220	4980
182.1	1250	4900
183.7	1320	5010
185.4	1380	5170
187.0	1420	5250
188.7	1390	5290
190.3	1310	5130
191.9	1250	5090
193.6	1290	5050
195.2	1260	5090
196.9	1200	5050
198.5	1210	5050
200.1	1200	4980
201.8	1260	5050
203.4	1280	5330
205.1	1440	5510
206.7	1470	5380
208.3	1180	5290
210.0	1120	5290
211.6	1110	5210
213.3	1170	5210
214.9	1190	5210
216.5	1200	5210
218.2	1260	5170
219.8	1230	5210
221.5	1240	5170
223.1	1290	5250
224.7	1250	5250
226.4	1230	5210
228.0	1300	5290
229.7	1290	5290
231.3	1280	5210
232.9	1310	5290
234.6	1350	5250
236.2	1350	5170
237.9	1380	5290
239.5	1360	5210
241.1	1290	5170
242.8	1300	5170
244.4	1300	5130
246.1	1300	5130

Table 5. Boring B-301, Suspension R1-R2 depths and P- and S_H-wave velocities

Depth (feet)	V_s (feet/sec)	V_p (feet/sec)
247.7	1340	5210
249.3	1360	5130
251.0	1340	5090
252.6	1230	5130
254.3	1230	5210
255.9	1250	5090
257.6	1270	5210
259.2	1330	5210
260.8	1360	5170
262.5	1250	5010
264.1	1150	4980
265.8	1150	4940
267.4	1170	5050
269.0	1180	5010
270.7	1190	5010
272.3	1180	5010
274.0	1180	4940
275.6	1140	4980
277.2	1130	4980
278.9	1180	5010
280.5	1150	5010
282.2	1120	5050
283.8	1100	4980
285.4	1080	5130
287.1	1150	5210
288.7	1320	5170
290.4	1330	5170
292.0	1320	5170
293.6	1360	5250
295.3	1390	5170
296.9	1370	5090
298.6	1360	5130
300.2	1540	5090
301.8	1390	5700
303.5	1680	6940
305.1	2070	7170
306.8	2120	6010
308.4	1720	5950
310.0	1800	5950
311.7	1790	5950
313.3	2150	6290
315.0	2340	6440
316.6	2040	6540
318.2	2070	6410
319.9	2700	6920
321.5	3060	7250
323.2	2150	6310
324.8	1920	5950
326.4	2310	5850
328.1	2340	6240
329.7	2230	6170
331.4	2160	6170
333.0	2160	6060
334.7	2250	6290
336.3	2230	6290
337.9	2030	6440
339.6	1880	5560
341.2	1840	5650
342.9	1890	5630
344.5	2140	5930
346.1	2260	6060
347.8	2040	5950
349.4	1870	5650
351.1	1780	5560
352.7	1810	5650
354.3	1880	5850
356.0	1970	5850
357.6	2070	5950
359.3	2150	6060
360.9	1980	5850
362.5	1850	5650
364.2	1860	5750
365.8	1860	5850
367.5	1870	5850
369.1	1890	5850
370.7	1840	5770
372.4	1860	5910
374.0	1980	5950
375.7	2030	5930
377.3	2030	5950
378.9	2070	6270
380.6	2040	6170
382.2	1980	6060
383.9	1990	5950
385.5	2050	5950
387.1	2070	6170
388.8	1900	6060
390.4	1790	5750

Table 6, continued Boring B-301, Suspension R1-R2 depths and P- and S_H-wave velocities

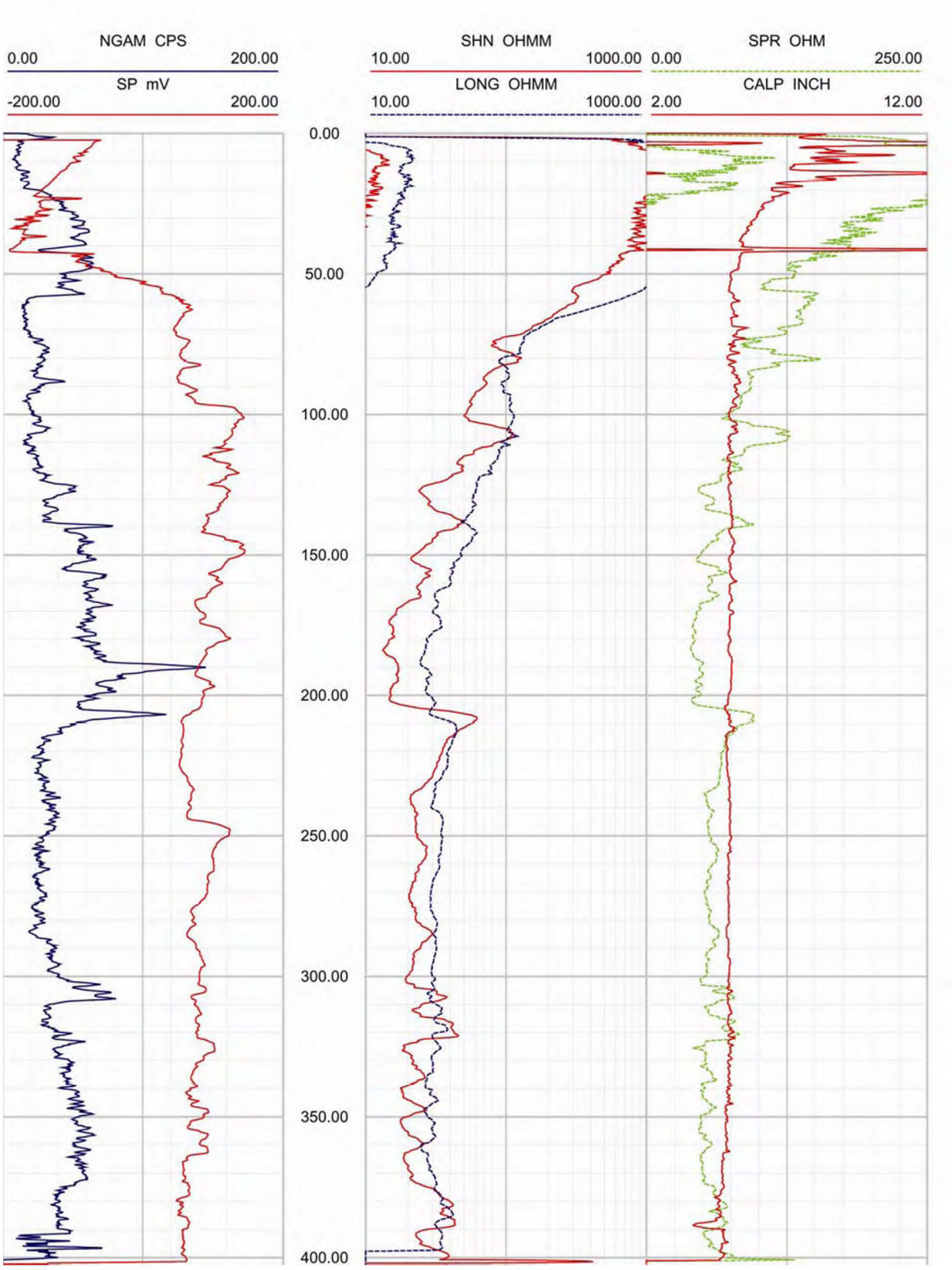

Figure 6. Boring B-301, Caliper, Natural gamma, Resistivity and SP logs

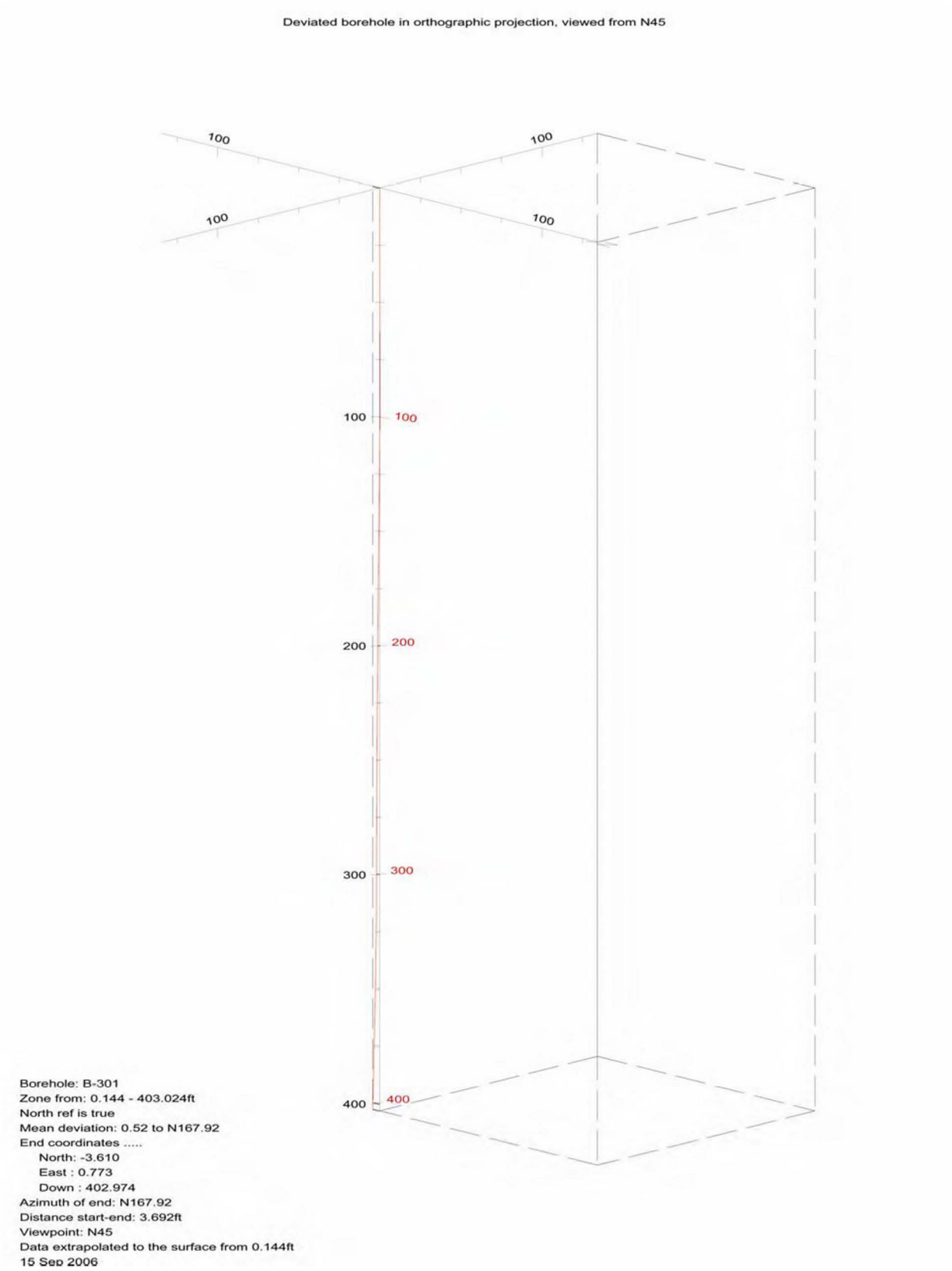

Figure 7. Boring B-301, Deviation Projection (dimensions in feet)

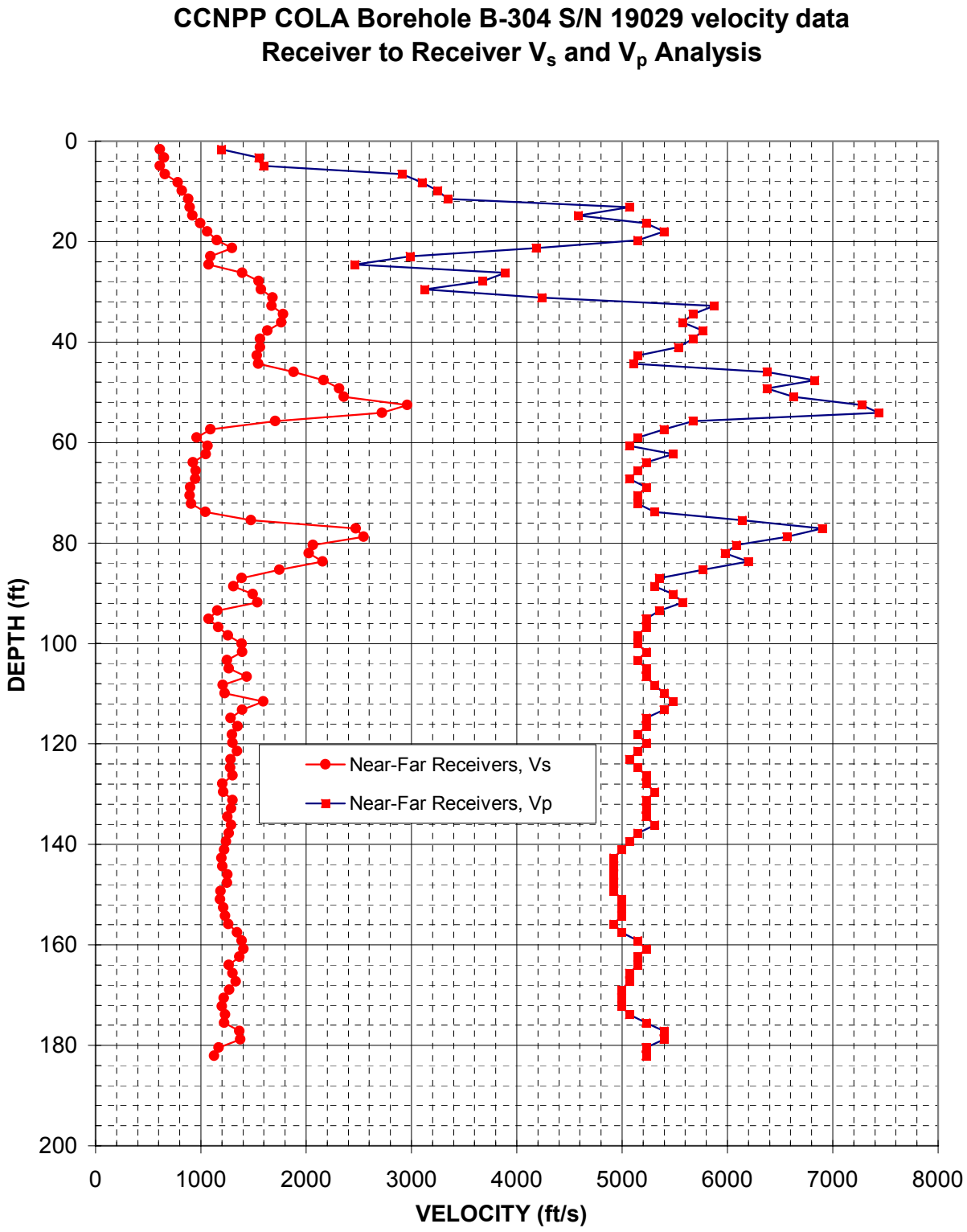

Figure 8. Boring B-304, S/N 19029, Suspension R1-R2 P- and S_H-wave velocities

Depth (feet)	V_s (feet/sec)	V_p (feet/sec)
1.6	610	1200
3.3	650	1550
4.9	610	1590
6.6	660	2910
8.2	780	3100
9.8	820	3250
11.5	880	3350
13.1	900	5070
14.8	920	4580
16.4	1000	5230
18.0	1060	5400
19.7	1150	5150
21.3	1300	4180
23.0	1090	2990
24.6	1070	2460
26.3	1390	3890
27.9	1550	3680
29.5	1570	3130
31.2	1680	4240
32.8	1670	5870
34.5	1780	5670
36.1	1770	5580
37.7	1630	5770
39.4	1560	5670
41.0	1560	5530
42.7	1530	5150
44.3	1550	5110
45.9	1880	6370
47.6	2170	6830
49.2	2320	6370
50.9	2360	6630
52.5	2960	7280
54.1	2720	7440
55.8	1710	5670
57.4	1090	5400
59.1	960	5150
60.7	1070	5070
62.3	1050	5490
64.0	920	5230
65.6	950	5150
67.3	950	5070
68.9	900	5230
70.5	900	5150
72.2	910	5150
73.8	1050	5310
75.5	1470	6140
77.1	2470	6900
78.7	2540	6560
80.4	2070	6080
82.0	2030	5980
83.7	2160	6200
85.3	1750	5770
86.9	1390	5350
88.6	1310	5310
90.2	1490	5490
91.9	1540	5580
93.5	1160	5350
95.1	1080	5230
96.8	1170	5230
98.4	1260	5150
100.1	1390	5150
101.7	1390	5230
103.4	1250	5150
105.0	1270	5230
106.6	1440	5230
108.3	1210	5310
109.9	1230	5400
111.6	1590	5490
113.2	1390	5400
114.8	1280	5230
116.5	1350	5230
118.1	1300	5150
119.8	1300	5230
121.4	1340	5150
123.0	1280	5070
124.7	1280	5150
126.3	1300	5230
128.0	1200	5230
129.6	1210	5310
131.2	1300	5230
132.9	1290	5230
134.5	1250	5230
136.2	1290	5310
137.8	1270	5150
139.4	1240	5070
141.1	1220	5000
142.7	1200	4920
144.4	1200	4920
146.0	1250	4920
147.6	1250	4920
149.3	1190	4920
150.9	1180	5000
152.6	1210	5000
154.2	1230	5000
155.8	1260	4920
157.5	1340	5000
159.1	1390	5150
160.8	1410	5230
162.4	1370	5150
164.0	1270	5150
165.7	1300	5070
167.3	1330	5070
169.0	1270	5000
170.6	1220	5000
172.2	1200	5000
173.9	1230	5070
175.5	1220	5230
177.2	1370	5400
178.8	1380	5400
180.5	1170	5230
182.1	1130	5230

Table 7. Boring B-304, S/N 19029 Suspension R1-R2 depths and P- and S_H-wave velocities

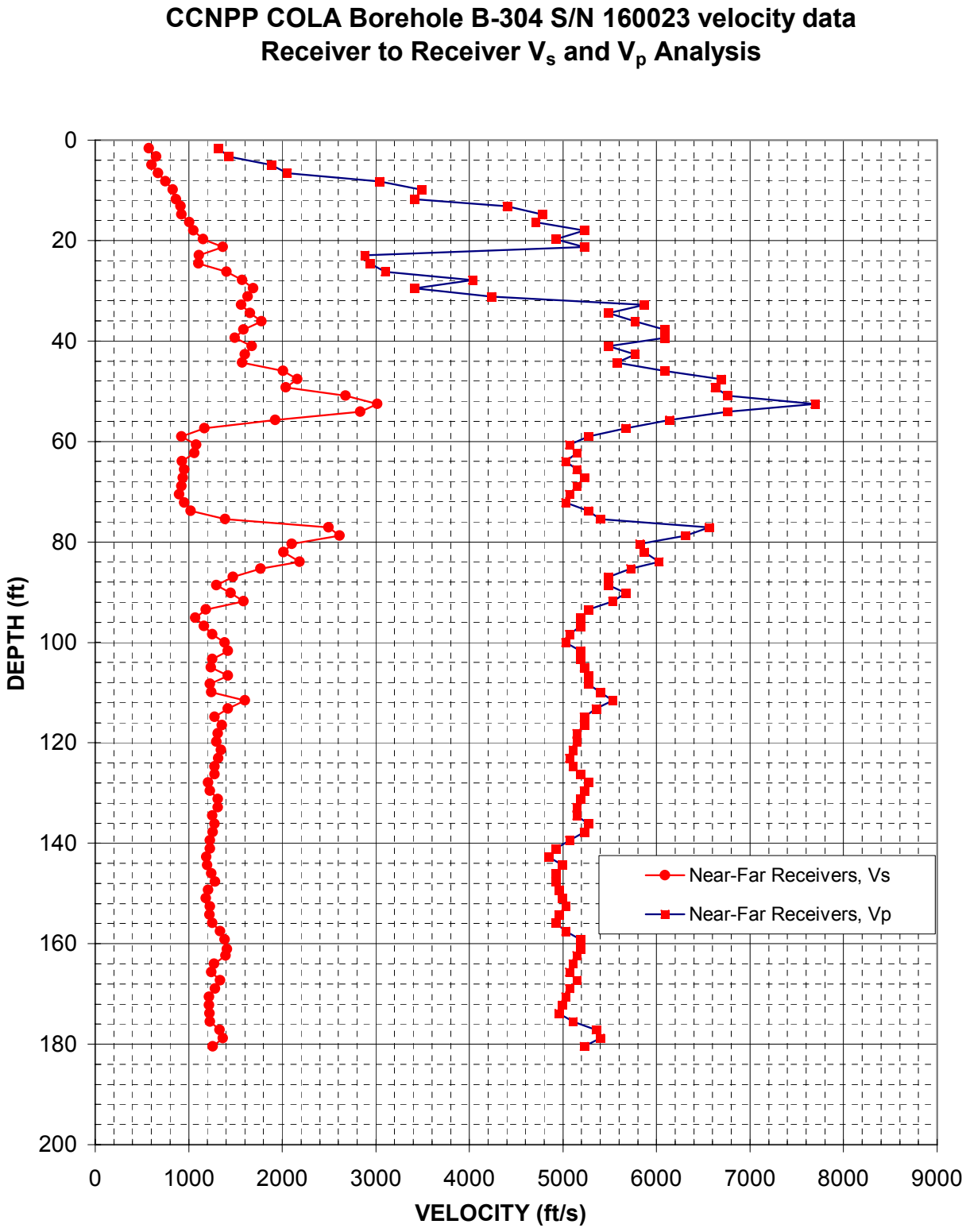

Figure 9. Boring B-304, S/N 160023, Suspension R1-R2 P- and S_H-wave velocities

Depth (feet)	V_s (feet/sec)	V_p (feet/sec)
1.6	580	1320
3.3	650	1430
4.9	600	1880
6.6	670	2050
8.2	750	3040
9.8	830	3490
11.8	870	3410
13.1	910	4400
14.8	920	4780
16.4	1010	4710
18.0	1050	5230
19.7	1150	4920
21.3	1370	5230
23.0	1110	2890
24.6	1100	2940
26.3	1410	3100
27.9	1570	4030
29.5	1690	3410
31.2	1630	4240
32.8	1560	5870
34.5	1660	5490
36.1	1780	5770
37.7	1590	6080
39.4	1490	6080
41.0	1670	5490
42.7	1600	5770
44.3	1570	5580
45.9	2010	6080
47.6	2160	6690
49.2	2040	6630
50.9	2680	6760
52.5	3020	7690
54.1	2840	6760
55.8	1920	6140
57.4	1170	5670
59.1	920	5270
60.7	1080	5070
62.3	1060	5150
64.0	930	5030
65.6	950	5150
67.3	940	5230
68.9	920	5150
70.5	900	5070
72.2	950	5030
73.8	1020	5270
75.5	1390	5400
77.1	2500	6560
78.7	2610	6310
80.4	2100	5820
82.0	2020	5870
84.0	2190	6030
85.3	1770	5720
86.9	1470	5490
88.6	1300	5490
90.2	1450	5670
91.9	1590	5530
93.5	1180	5270
95.1	1070	5190
96.8	1160	5190
98.4	1250	5070
100.1	1380	5030
101.7	1420	5190
103.4	1250	5190
105.0	1240	5230
106.6	1420	5270
108.3	1230	5270
109.9	1240	5400
111.6	1600	5530
113.2	1420	5350
114.8	1280	5230
116.5	1350	5230
118.1	1310	5150
119.8	1300	5150
121.4	1340	5110
123.0	1320	5070
124.7	1280	5110
126.3	1280	5190
128.0	1210	5270
129.6	1230	5230
131.2	1310	5190
132.9	1310	5150
134.5	1250	5150
136.2	1280	5270
137.8	1260	5230
139.4	1230	5070
141.1	1230	4920
142.7	1190	4850
144.4	1200	5000
146.0	1240	4920
147.6	1280	4920
149.3	1210	4960
150.9	1180	5000
152.6	1230	5030
154.2	1220	4960
155.8	1250	4920
157.5	1340	5030
159.1	1380	5190
161.1	1410	5190
162.4	1390	5150
164.0	1270	5110
165.7	1240	5070
167.3	1340	5150
169.0	1280	5070
170.6	1220	5030
172.2	1220	5000
173.9	1220	4960
175.5	1230	5110
177.2	1330	5350
178.8	1370	5400
180.5	1260	5230

Table 8. Boring B-304, S/N 160023 Suspension R1-R2 depths and P- and S_H-wave velocities

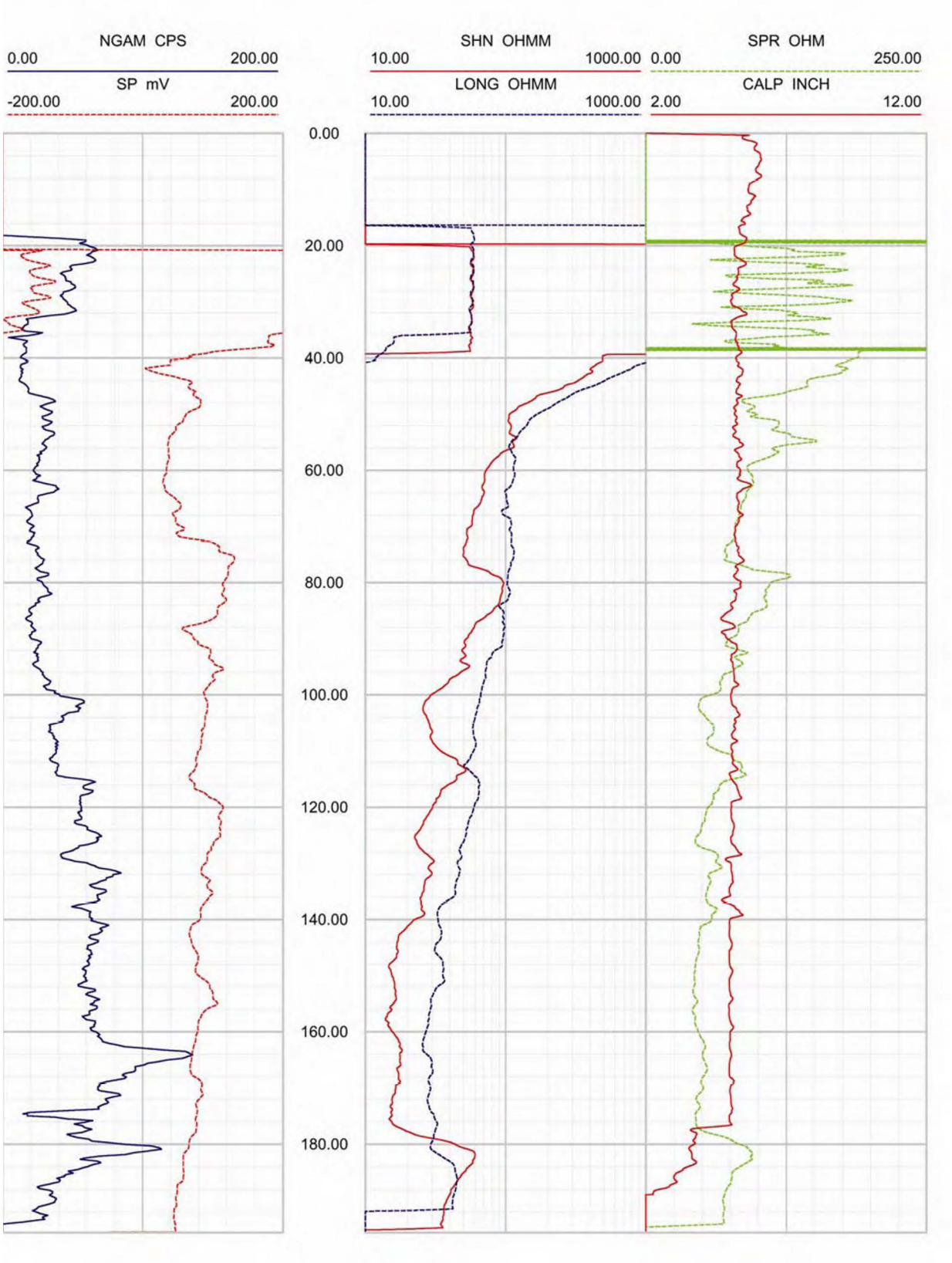

Figure 10. Boring B-304, Caliper, Natural gamma, Resistivity and SP logs